Binuclear Activation of Cumulenes: Roles of the Adjacent Metals and the Cumulene Binding Mode in the Activation Process

Dusan Ristic-Petrovic, D. Jason Anderson, Jeffrey R. Torkelson, Michael J. Ferguson,‡ Robert McDonald,‡ and Martin Cowie*

Department of Chemistry, University of Alberta, Edmonton, Alberta, Canada T6G 2G2

Received February 18, 2005

The binuclear complex $[Ir_2(CH_3)(CO)(\mu\text{-}CO)(dppm)_2][CF_3SO_3]$ (**1**; dppm = μ-$Ph_2PCH_2PPh_2$) reacts with allene and methylallene to ultimately yield the vinylcarbene products $[Ir_2H(CO)_2(\mu\text{-}\eta^1\text{:}\eta^3\text{-}HCC(CH_3)C(H)R)(dppm)_2][CF_3SO_3]$ (R = H (**6**), CH_3 (**7**)). Monitoring the reactions by NMR spectroscopy (^1H, ^{13}C, ^{31}P) between −78 °C and ambient temperature allows the observation of several intermediates in each of these transformations in which the allene moves from an η^2 binding site on one metal, through an η^1:η^1-bridging geometry in which the cumulene is coordinated through the "H_2C=C" moiety, to an η^1:η^3-bridging geometry in which the central carbon of the cumulene is σ-bound to one metal, adjacent to the methyl ligand, while the three cumulene carbons are η^3-bound to the adjacent metal. We propose that formation of the respective vinyl carbene products results from migration of the methyl ligand to the central cumulene carbon followed by activation of a cumulene C−H bond. 1,1-Dimethylallene reacts with **1** at −78 °C to yield a methylene hydride product containing an η^2-bound cumulene on one metal, much as observed for the first products in the allene and methylallene reactions. Upon warming, this intermediate isomerizes to the final product containing a methyl ligand on one metal and an η^2-bound cumulene on the other. No cumulene-bridged products are observed with this disubstituted allene. 1,1-Difluoroallene also yields a methylene hydride product at −78 °C, which is analogous to the first species observed in all cases noted above. In this case, warming results in movement of the cumulene to an η^1:η^1-bridging position in which this group binds to the metals via the "H_2C=C" moiety. Unlike the transformations observed with allene and methyl allene, difluoroallene undergoes no additional transformations as the temperature is raised. A rationalization of these transformations is presented together with a perspective on how the cumulene ligand moves over the dimetallic framework leading to the final products.

Introduction

Chemistry occurring on metal surfaces is notoriously difficult to study,[1a,b] and it is especially difficult to obtain detailed information about the natures of surface-bound organic fragments and their roles in the facile transformations occurring on catalyst surfaces. Fortunately, information about the possible natures of these surface-bound fragments can be obtained through analogies with well-defined organometallic complexes, based on the concept, championed by the late E. L. Muetterties and others,[1] that chemical transformations occurring on metal surfaces and in metal complexes are fundamentally the same. The most obvious difference between metal surfaces and mononuclear metal complexes (apart from the well-defined geometry of ancillary ligands surrounding the metal in the latter) is the presence of adjacent metal centers in the former. So although the chemistry occurring in each environment (surface and single metal) is fundamentally no different, it nevertheless seems intuitively clear that the presence of adjacent metals should give rise to some degree of reactivity differences compared to those occurring at single metals. Certainly, the existence of bridged-ligand binding modes is only possible in complexes containing adjacent metals, and one might assume that such bonding should give rise to differences in reactivity (either subtle or dramatic) compared to that of terminally bound groups.[2]

Although a large number of polymetallic complexes have been studied,[3] surprisingly little is understood about the roles of the adjacent metals in the activation

* Corresponding author. E-mail: martin.cowie@ualberta.ca.
‡ X-ray Crystallography Laboratory.

(1) (a) Zaera, F. *Chem. Rev.* **1995**, *95*, 2651. (b) Muetterties, E. L. *Pure Appl. Chem.* **1982**, *54*, 83. (b) Muetterties, E. L.; Rhodin, T. N.; Band, E.; Brucker, C. F.; Pretzer, W. R. *Chem. Rev.* **1979**, *79*, 91. (c) Muetterties, E. L. *Chem. Soc. Rev.* **1982**, *11*, 283. (d) Marks, T. J. *Acc. Chem. Res.* **1992**, *25*, 57. (e) Schmid, G. *Chem. Rev.* **1992**, *92*, 1709. (f) Schmid, G., Ed. *Clusters and Colloids*; VCH: Weinheim, 1994. (g) Johnson, B. F. G. *J. Mol. Catal.* **1994**, *86*, 51.

(2) (a) Shriver, D. F.; Sailor, M. J. *Acc. Chem. Res.* **1988**, *21*, 374. (b) Xiao, F.-S.; Fukuoka, A.; Ichikawa, M. *J. Catal.* **1992**, *138*, 206. (c) Araki, M.; Ponec, V. *J. Catal.* **1976**, *44*, 439. (d) Vites, J.; Housecroft, C. E.; Eigenbrot, C.; Buhl, M.; Long, G. J.; Fehlner, T. P. *J. Am. Chem. Soc.* **1985**, *107*, 8147. (e) Horvitz, C. P.; Shriver, D. G. *J. Am. Chem. Soc.* **1985**, *107*, 8147.

(3) See for example: (a) Braunstein, P. In *Perspectives in Coordination Chemistry*; Williams, A. F.; Floriani, C.; Merbach, A. E., Eds.; Verlag Helvetica Chim. Acta: Basel, 1992; p 67. (b) Shriver, D. F.; Kaesz, H. D.; Adams, R. D. *The Chemistry of Metal Cluster Complexes*; VCH: Weinheim, 1990. (c) Stone, F. G. A. *Angew. Chem., Int. Ed. Engl.* **1984**, *23*, 89.

10.1021/om0580102 CCC: $30.25
Publication on Web 06/22/2005

Scheme 1

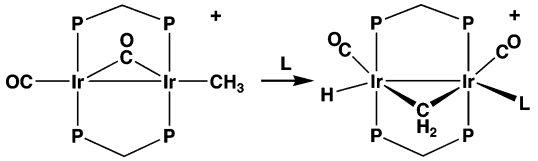

of substrate molecules. Our approach to studying such processes has involved a series of binuclear, diphosphine-bridged complexes in which an abundance of NMR-active nuclei (^{31}P, ^{19}F, ^{13}C, ^{1}H) allows an in-depth investigation of solution intermediates, often allowing the determination of substrate and ancillary ligand coordination modes throughout much of the activation process.[4] Other groups have taken a similar approach using related diphosphine-bridged systems.[5]

One example of unusual reactivity initiated by the presence of an adjacent metal is the facile C−H activation of a methyl group at one metal upon ligand addition at the adjacent metal, as was observed in reactions of $[Ir_2(CH_3)(CO)_2(dppm)_2][CF_3SO_3]$ (**1**; dppm = μ-$Ph_2PCH_2PPh_2$) diagrammed in Scheme 1.[4d,6] Although α-hydrogen elimination involving a methyl ligand at an early-metal center is common,[7] such C−H activation at a single-site, late-metal complex is not. In the example given above, the presence of an adjacent metal induces reactivity not routinely observed with single metals. As part of a strategy to exploit the above C−H bond activation in subsequent carbon−carbon bond formation, we have investigated the addition of unsaturated hydrocarbons to compound **1**, in attempts to induce coupling between these unsaturated substrates and the resulting bridging methylene group.[4d,8−10] Numerous examples involving insertion of olefins,[11] alkynes,[12] and cumulenes[13] into the metal−carbon bonds of bridging methylene groups have been reported, and we earlier reported the reactions of **1** with a series of alkynes[8,9] and olefins.[4d,10]

In this paper we report the reactivity of **1** with a series of cumulenes in order to determine if the C−H activation process reported in Scheme 1 has a role in subsequent C−C bond formation. A preliminary report of some of this chemistry has appeared.[8]

Experimental Section

General Comments. All solvents were dried (using appropriate drying agents), distilled before use, and stored under dinitrogen. Deuterated solvents used for NMR experiments were freeze−pump−thaw degassed (three cycles) and stored under nitrogen or argon over molecular sieves. Reactions were carried out under argon using standard Schlenk techniques, and compounds that were used as solids were purified by recrystallization. Prepurified argon and nitrogen were purchased from Linde, carbon-13 enriched CO (99%) was supplied by Isotec Inc., and methylallene was supplied by Fluka. All gases were used as received, and all other reagents were purchased from Aldrich and were used as received, except as noted. The compound $[Ir_2(CH_3)(CO)(\mu\text{-}CO)(dppm)_2][CF_3SO_3]$ (**1**) was prepared as previously reported.[6] The perdeuteromethyl analogue **1-*d*$_3$** was also prepared by the literature method, except that methyl-d_3 trifluoromethanesulfonate was reacted with $[Ir_2(CO)_3(dppm)_2]$, and the trimethylamine *N*-oxide used to remove one of the carbonyls was purified to avoid incorporation of protium into the methyl group of the product, by first recrystallizing commercial anhydrous trimethylamine *N*-oxide from D_2O and then subliming it in vacuo.

Proton NMR spectra were recorded on Varian Unity 400, 500, or 600 spectrometers or on a Bruker AM400 spectrometer. Carbon-13 NMR spectra were recorded on Varian Unity 400 or Bruker AM300 spectrometers. Phosphorus-31 and fluorine-19 NMR spectra were recorded on Varian Unity 400 or Bruker AM400 spectrometers. Two-dimensional NMR experiments (COSY, ROESY, TOCSY, and $^{13}C-^{1}H$ HMQC) were obtained on Varian Unity 400 or 500 spectrometers. NMR spectral data for all compounds are given in Table 1, whereas IR data, when available, are given with the details of preparation.

1,1-Difluoroallene was prepared using a modification of a published procedure,[14] in which a solution of 20 μL of 2-bromo-3,3,3-trifluoro-1-propene in 2 mL of Et_2O in a round-bottom flask was cooled to −90 °C in a heptane/liquid N_2 bath. To this was added dropwise 100 μL of a 1.6 M solution of *n*-butyllithium in hexanes, followed by stirring of the solution at this temperature for 10 min. The −90 °C bath was replaced

(4) See for example: (a) George, D. S. A.; Hilts, R. W.; McDonald, R.; Cowie, M. *Organometallics* **1999**, *18*, 5330. (b) George, D. S. A.; Hilts, R. W.; McDonald, R.; Cowie, M. *Inorg. Chim. Acta* **2000**, *300−302*, 353. (c) Trepanier, S. J.; McDonald, R.; Cowie, M. *Organometallics* **2003**, *22*, 2638. (d) Ristic-Petrovic, D.; Anderson, D. J.; Torkelson, J. R.; McDonald, R.; Cowie, M. *Organometallics* **2003**, *22*, 4647. (e) Rowsell, B. D.; McDonald, R.; Cowie, M. *Organometallics* **2004**, *23*, 3873.

(5) See for example: (a) Johnson, K. A.; Vashan, M. D.; Moassen, B.; Warmka, B. K.; Gladfelter, W. L. *Organometallics* **1995**, *14*, 461. (b) Oldham, S. M.; Houlis, J. F.; Sleigh, C. J.; Duckett, S. B.; Eisenberg, R. *Organometallics* **2000**, *19*, 2985. (c) Gao, Y.; Hennings, M. C.; Puddephatt, R. J. *Organometallics* **2001**, *20*, 1882. (d) Veige, A. S.; Gray, T. G.; Nocera, D. G. *Inorg. Chem.* **2005**, *44*, 17. (e) Rashidi, M.; Kamali, K.; Jennings, M. C.; Puddephatt, R. J. *J. Organomet. Chem.* **2005**, *690*, 1600. (f) Alvarez, M. A.; Anaya, Y.; García, M. E.; Ruiz, M. A.; Vaissermann, J. *Organometallics* **2005**, *24*, 2452.

(6) Torkelson, J. R.; Antwi-Nsiah, F. H.; McDonald, R.; Cowie, M.; Pruis, J. G.; Jalkanen, K. J.; DeKock, R. L. *J. Am. Chem. Soc.* **1999**, *121*, 3666.

(7) Collman, J. P.; Hegedus, L. S.; Norton, J. R.; Finke, R. G. *Principles and Applications of Organotransition Metal Chemistry*; University Science Books: Mill Valley, CA. 1987; Chapter 3.

(8) Torkelson, J. R.; McDonald, R.; Cowie, M. *J. Am. Chem. Soc.* **1998**, *120*, 4047.

(9) Torkelson, J. R.; McDonald, R.; Cowie, M. *Organometallics* **1999**, *18*, 4134.

(10) Ristic-Petrovic, D.; Torkelson, J. R.; Hilts, R. W.; McDonald, R.; Cowie, M. *Organometallics* **2000**, *19*, 4432.

(11) (a) Howard, T. R.; Lee, J. B.; Grubbs, R. H. *J. Am. Chem. Soc.* **1980**, *102*, 6876. (b) Lee, J. B.; Gajola, G. J.; Schaefer, W. P.; Howard, T. R.; Ikariya, T.; Straus, D. A.; Grubbs, R. H.; *J. Am. Chem. Soc.* **1981**, *103*, 7358. (c) Motyl, K. M.; Norton, J. R.; Schauer, C. K.; Anderson, O. P. *J. Am. Chem. Soc.* **1982**, *104*, 7325. (d) Sumner, C. E., Jr.; Riley, P. E.; David, R. E.; Pettit, R. *J. Am. Chem. Soc.* **1980**, *102*, 1752. (e) Theopold, K. H.; Bergman, R. G. *J. Am. Chem. Soc.* **1981**, *103*, 2489. (f) Kao, S. C.; Thiel, C. H.; Pettit, R. *Organometallics* **1983**, *2*, 914.

(12) (a) Dyke, A. F.; Knox, S. A. R.; Naish, P. J.; Taylor, G. E. *J. Chem. Soc., Chem. Commun.* **1980**, 803. (b) Gracey, B. P.; Knox, S. A. R.; Macpherson, K. A.; Orpen, A. G.; Stobart, S. R. *J. Chem. Soc., Dalton Trans.* **1985**, 1935. (c) Sumner, C. E.; Collier, J. A.; Pettit, R. *Organometallics* **1982**, *1*, 1350. (d) Akita, M.; Hua, R.; Nakanishi, S.; Tanaka, M.; Moro-oka, Y. *Organometallics* **1987**, *16*, 5572. (e) Adams, P. Q.; Davis, D. L.; Dyke, A. F.; Knox, S. A. R.; Mead, K. A.; Woodward, P. *J. Chem. Soc., Chem. Commun.* **1983**, 222. (f) Colborn, R. E.; Dyke, A. F.; Knox, S. A. R.; Macpherson, K. A.; Orpen, A. G. *J. Organomet. Chem.* **1982**, *239*, C15. (g) Colborn, r. E.; Davies, D. L.; Dyke, A. F.; Knox, S. A. R.; Mead, K. A.; Orpen, A. G.; Guerchais, J. E.; Roue, J. *J. Chem. Soc., Dalton Trans.* **1989**, 1799. (h) Dennett, J. N. L. Ph.D. Thesis, Chapter 4, University of Bristol, Bristol, UK, 2000. (i) Kaneko, Y.; Suzuki, T.; Isobe, K.; Maitlis, P. M. *J. Organomet. Chem.* **1998**, *554*, 155. (j) Navarre, D.; Parlier, A.; Rudler, H.; Daran, J. C. *J. Organomet. Chem.* **1987**, *322*, 103. (k) Levisalles, J.; Rose-Munch, F.; Rudler, H.; Daran, J. C.; Dranzee, Y.; Jeannin, Y. *J. Chem. Soc., Chem. Commun.* **1981**, 152.

(13) (a) Fildes, M. J.; Knox, S. A. R.; Orpen, A. G.; Turner, M. L.; Yates, M. I. *J. Chem. Soc., Chem. Commun.* **1989**, 1680. (b) Chetcuti, M. J.; Fanwick, P. E.; Grant, B. E. *Organometallics* **1991**, *10*, 3003. (c) Chokshi, A.; Rowsell, B. D.; Trepanier, S. J.; Ferguson, M. J.; Cowie, M. *Organometallics* **2004**, *23*, 4759.

(14) Drakesmith, F. G.; Stewart, O. J.; Tarrant, P. *J. Org. Chem.* **1967**, *33*, 280.

Table 1. NMR Data for the Compounds[a,b]

compound[c]	$\delta(^{31}P\{^1H\})$[d]	$\delta(^1H)$[e,f]	$\delta(^{13}C\{^1H\})$[e]
$[Ir_2(H)(CO)_2(anti\text{-}\eta^2\text{-}H_2C{=}C{=}CH_2)(\mu{-}CH_2)(dppm)_2]^+$ (**2a**) and $[Ir_2(H)(CO)_2(syn\text{-}\eta^2\text{-}H_2C{=}C{=}CH_2)(\mu{-}CH_2)(dppm)_2]^+$ (**2b**)	−1.6 (m, 4P), −6.7 (m, 2P), −9.0 (m, 2P)	4.99 (b, 4H), −12.25 (b, 2H)	190.3 (b), 189.3 (b), 176.1 (b), 174.8 (b)
$[Ir_2(CH_3)(\mu\text{-}H_2C{=}C{=}CH_2)(CO)_2(dppm)_2]^+$ (**2c**)	25.3 (m, 2P), −5.5 (m, 2P)	6.06 (s, 1H), 4.01 (s, 1H), 3.62 (m, 2H), 3.44 (m, 2H), 2.46 (t, 2H, $^3J_{PH}$ = 11.8 Hz), 0.18 (t, 3H, $^3J_{PH}$ = 6.4 Hz)	192.4 (t, $^2J_{PC}$ = 8.8 Hz), 186.2 (t, $^2J_{PC}$ = 6.0 Hz)
$[Ir_2(CH_3)(\eta^2\text{-}H_2C{=}C{=}CH_2)(CO)_2(dppm)_2]^+$ (**2d**)	19.5 (m, 2P), 2.5 (m, 2P)	5.61 (b, 1H), 4.81 (b, 1H), 4.24 (b, 2H), 3.54 (m, 4H), 1.23 (t, 3H, $^3J_{PH}$ = 8.6 Hz)	206.6 (b), 206.2 (b)
$[Ir_2(CH_3)(CO)_2(\mu\text{-}\eta^1{:}\eta^3\text{-}H_2C{=}C{=}CH_2)(dppm)_2]^+$ (**2e**)	−15.7 (m)	5.46 (m, 2H), 5.09 (m, 2H), 4.23 (b, 2H), 3.52 (b, 2H), 1.18 (t, 3H, $^3J_{PH}$ = 5 Hz)	179.2(t), 171.2 (b), 127.3 (b), 61.3 (m), −31.1 (t, $^2J_{PC}$ = 3.3 Hz)
$[Ir_2(H)(CO)_2(anti\text{-}\eta^2\text{-}H_2C{=}C{=}CH(CH_3))(\mu\text{-}CH_2)(dppm)_2]^+$ (**3a**) and $[Ir_2(H)(CO)_2(syn\text{-}\eta^2\text{-}H_2C{=}C{=}CH(CH_3))(\mu\text{-}CH_2)(dppm)_2]^+$ (**3b**)	−0.4 (m, 2P), −6.9 (m, 2P) −2.6 (m, 2P), −8.0 (m, 2P)	−12.0 (b, 1H), −12.6 (b, 1H)	189.9 (b), 189.5 (b), 176.5 (b), 175.9 (b)
$[Ir_2(CH_3)(CO)_2(\mu\text{-}H_2C{=}C{=}CH(CH_3))(dppm)_2]^+$ (**3c**)	27.6 (m, 2P), −5.9 (m, 2P)	3.80 (s, 1H), 3.45 (m, 4H), 2.07 (t, 2H, $^3J_{PH}$ = 11.4 Hz), 1.76 (d, 3H, $^3J_{HH}$ = 3.0 Hz), 0.23 (t, 3H, $^3J_{PH}$ = 6.6 Hz)	191.7 (t, $^2J_{PC}$ = 8.0 Hz), 186.4 (b)
$[Ir_2(CH_3)(CO)_2(\mu\text{-}H_2C{=}C{=}CH(CH_3))(dppm)_2]^+$ (**3d**)	19.9 (m, 2P), 2.9 (m, 2P)	4.75 (m, 1H), 1.25 (t, 3H, $^3J_{PH}$ = 8.5 Hz), 0.90 (d, $^3J_{HH}$ = 3.4 Hz)	208.2 (b), 207.3 (b)
$[Ir_2(CH_3)(CO)_2(\mu\text{-}\eta^1{:}\eta^3\text{-}H_2C{=}C{=}C(H)CH_3)(dppm)_2]^+$ (**3e**)	−14.2 (m, 1P), −16.2 (m, 2P), −17.5 (m, 1P)	5.79 (m, 1H), 5.38 (m, 1H), 5.19 (m, 1H), 5.17 (m, 1H), 4.87 (m, 1H), 4.70 (qm, 1H, $^3J_{HH}$ = 6 Hz), 3.78 (m, 1H), 1.16 (t, 3H, $^3J_{PH}$ = 5 Hz), 1.07 (t, 3H, $^3J_{HH}$ = 6 Hz, $^4J_{PH}$ = 6 Hz)	179.4 (t), 170.9 (b), 78.7 (m), 55.6 (m), 18.6(m) −32.2 (t)
$[Ir_2(H)(CO)_2(\eta^2\text{-}H_2C{=}C{=}C(CH_3)_2)(\mu\text{-}CH_2)(dppm)_2]^+$ (**4a**)	1.3 (m, 2P), −13.7 (m, 2P)	5.96 (b, 2H), 5.16 (b, 2H), 3.48 (b, 2H), 1.90 (b, 2H), 1.13 (b, 3H), 0.19 (b, 3H), −12.1 (b, 1H)	191.1 (b), 178.2 (b)
$[Ir_2(CH_3)(CO)_2(\eta^2\text{-}H_2C{=}C{=}C(CH_3)_2)(dppm)_2]^+$ (**4d**)	18.3 (m, 2P), 0.3 (m, 2P)	3.48 (m, 2H), 3.19 (m, 2H), 1.58 (s, 2H), 1.22 (b, 3H), 1.17 (t, $^3J_{PH}$ = 8.5 Hz, 3H), 0.98 (b, 3H)	206.4 (t, $^2J_{PC}$ = 6.9 Hz), 204.8 (t, $^2J_{PC}$ = 7.0 Hz)
$[Ir_2(H)(CO)_2(\eta^2\text{-}H_2C{=}C{=}CF_2)(\mu\text{-}CH_2)(dppm)_2]^+$ (**5a**)[g]	−2.5 (m, 2P), −7.1 (m, 2P)	5.22 (b, 2H), 5.02 (b, 2H), 3.22 (b, 2H), 1.62 (b, 2H), −12.5 (b, 1H)	187.4 (b), 174.4 (m)
$[Ir_2CH_3(CO)_2(\mu\text{-}H_2C{=}C{=}CF_2)(dppm)_2]^+$ (**5c**)[g]	19.5 (m, 2P), −2.6 (m, 2P)	3.92 (m, 2H), 3.57 (m, 2H), 2.51 (t, 2H, $^3J_{PH}$ = 12.0 Hz), 0.10 (t, 3H, $^3J_{PH}$ = 8.6 Hz)	192.4 (m), 183.0 (t, $^2J_{PC}$ = 7.0 Hz)
$[Ir_2H(CO)_2(\mu\text{-}\eta^1{:}\eta^3\text{-}HCC(Me)CH_2)(dppm)_2]^+$ (**6**)	−5.1 (m 2P), −30.2 (m, 1P), −32.4 (m, 1P)	8.72 (m, 1H), 5.93 (m, 1H), 4.60 (m, 1H), 3.44 (m, 1H), 3.43 (m, 1H), 3.11 (m, 1H), 2.89 (d, 3H), −11.38 (m, 1H)	
$[Ir_2H(CO)_2(\mu\text{-}\eta^1{:}\eta^3\text{-}HCC(Me)CHMe)(dppm)_2]^+$ (**7a**)	−5.8 (m), −6.0 (m), −34.3 (m), −37.8 (m)	8.79 (m, 1H), 7.12 (m, 1H), 5.83[h] (m, 1H), 4.60 (m, 1H), 3.78 (m, 1H), 3.29 (m, 1H), 2.72 (d, 3H), 1.42 (bm, 3H), −11.25 (m, 1H)	
$[Ir_2H(CO)_2(\mu\text{-}\eta^1{:}\eta^3\text{-}HCC(Me)CHMe)(dppm)_2]^+$ (**7b**)	−7.6 (m, 2P), −30.8 (m, 1P), −37.9 (m, 1P)	8.96 (m, 1H), −11.18 (m, 1H)	

[a] NMR abbreviations: s = singlet, d = doublet, t = triplet, m = multiplet, b = broad. [b] NMR data CD_2Cl_2 unless otherwise stated. [c] In all cases trifluoromethanesulfonate is the accompanying anion. [d] $^{31}P\{^1H\}$ chemical shifts are referenced vs external 85% H_3PO_4. [e] ^1H and ^{13}C chemical shifts are referenced vs external TMS. [f] Chemical shifts for the phenyl hydrogens are not given in the ^1H data. [g] ^{19}F chemical shifts are referenced vs external $CFCl_3$. Resonances for **5a**: δ -79.2 (s, 3F), −80.5 (d, $^2J_{FF}$ = 84 Hz, 1F), −97.5 (d, $^2J_{FF}$ = 84 Hz, 1F); for **5b**: δ -79.2 (s, 3F), −66.9 (d, $^2J_{FF}$ = 56 Hz, 1F), −81.6 (d, $^2J_{FF}$ = 56 H, 1F). [h] Most ^1H NMR signals for **7a** and **7b** overlap so could not be clearly identified. Those identified as due to **7a** are based on a comparison with those of an authentic sample prepared by an alternate route.

by a chlorobenzene/liquid N_2 bath (ca. −40 °C), resulting in the evolution of 1,1-difluoroallene gas.

Preparation of Compounds. (a) [$Ir_2(CH_3)(CO)_2(\mu\text{-}\eta^1{:}\eta^3\text{-}H_2C{=}C{=}CH_2)(dppm)_2][CF_3SO_3]$ (2e). A solution of compound **1** (50 mg, 0.036 mmol) in 5 mL of CH_2Cl_2 was cooled to −78 °C, and allene was passed through the solution for 1 min, causing an immediate color change from red to light yellow. The solution was stirred for 30 min at −78 °C and then warmed to room temperature and stirred for 1 h. The solvent was reduced to ca. 2 mL, and a yellow powder was precipitated with addition of 10 mL of Et_2O. The isolated solid was washed with Et_2O (2 × 10 mL) and dried under vacuum. Yield: 73%. Anal. Calcd for $Ir_2SP_4F_3O_5C_{57}H_{51}$: C, 48.43; H, 3.64. Found: C, 48.23; H, 3.50. HRMS *m/z* calcd for $Ir_2P_4O_2C_{56}H_{51}$: 1265.2098. Found: 1265.2108. IR: ν(CO) = 1998(s).

(b) [$Ir_2(CH_3)(CO)_2(\mu\text{-}\eta^1{:}\eta^3\text{-}H_2C{=}C{=}C(H)CH_3)(dppm)_2][CF_3SO_3]$ (3e). A solution of compound **1** (50 mg, 0.036 mmol) in 5 mL of CH_2Cl_2 was cooled to 0 °C, and methylallene was then passed through the solution for 1 min, causing an immediate color change from red to light yellow. The solution was stirred for 30 min at 0 °C and then warmed to room temperature and stirred for 1 h, during which time the solution changed to bright yellow. The solvent was reduced to ca. 2 mL, and a bright yellow powder was precipitated with addition of 10 mL of Et_2O. The isolated solid was washed with Et_2O (2 × 10 mL) and dried under vacuum. Yield: 63%. NMR characterization of **3e** showed it to contain approximately 10% unidentified impurities from which the desired product could not be separated. HRMS *m/z* calcd for $Ir_2P_4O_2C_{57}H_{53}$: 1279.2255. Found: 1279.2254. IR: ν(CO) = 1994(s).

(c) [$Ir_2(CH_3)(CO)_2(\eta^2\text{-}H_2C{=}C{=}C(CH_3)_2)(dppm)_2][CF_3SO_3]$ (4d). Dimethylallene (3.2 μL, 0.033 mmol) was added to a solution of compound **1** (45 mg, 0.033 mmol) in 5 mL of CH_2Cl_2 at −78 °C, and the solution was stirred for 10 min, during which time the solution changed to bright yellow. The solution was warmed to room temperature, the solvent was reduced to ca. 2 mL, and a bright yellow powder was precipitated with addition of 10 mL of Et_2O. The isolated solid was washed with Et_2O (2 × 10 mL) and dried under vacuum. Yield: 55%. HRMS *m/z* calcd for $Ir_2P_4O_2C_{58}H_{55}$: 1293.2411. Found: 1293.2415. IR: ν(CO) = 1793(m), 1963(br).

(d) [$Ir_2(CH_3)(CO)_2(\mu\text{-}\eta^1{:}\eta^1\text{-}H_2C{=}C{=}CF_2)(dppm)_2][CF_3SO_3]$ (5c). The 1,1-difluoroallene gas that was evolved in the reaction described earlier was passed into a solution of 50 mg (0.036 mmol) of compound **1** in 10 mL of CH_2Cl_2 at −78 °C, resulting in the solution color changing to magenta. The cooling bath was removed, causing the solution to slowly turn orange as it warmed. The solution volume was reduced to ca. 2 mL, and addition of 10 mL of Et_2O resulted in the precipitation of a brick-red solid, which was dried in vacuo overnight, yielding 39 mg (83%) of the compound. HRMS *m/z* calcd for $Ir_2P_4F_2O_2C_{56}H_{49}$: 1301.1910. Found: 1301.1918. IR: ν(CO) = 1992(m), 1949(w).

(e) [$Ir_2(H)(CO)_2(\mu\text{-}\eta^1{:}\eta^3\text{-}HCC(Me){=}CH_2)(dppm)_2][CF_3SO_3]$ (6). Compound **2e** (20 mg, 0.014 mmol) was dissolved in 10 mL of CH_2Cl_2 and stirred for 7 days. The solvent volume was reduced to ca. 2 mL, and a yellow powder was obtained on addition of 10 mL of Et_2O. The solid was isolated, washed with Et_2O (2 × 10 mL), and dried under vacuum. NMR spectra showed that yields of **6** were variable, with the highest observed being 80%, among a mixture of other related uncharacterized products. Compound **6** was characterized by comparison of its ^1H and ^{31}P NMR spectra with those of closely related compounds that had been previously characterized.[9]

(f) [$Ir_2(H)(CO)_2(\mu\text{-}\eta^1{:}\eta^3\text{-}HCC(Me){=}CHMe)(dppm)_2][CF_3SO_3]$ (7a/7b). Leaving a solution of **3e** for approximately 5 days resulted in 50% conversion to a mixture of isomers **7a** and **7b** in an approximate 2:1 ratio, together with minor amounts of **1** and unidentified decomposition products. These isomers were never obtained as pure species. Isomer **7a** was identified by comparison of its NMR spectral parameters with those of the authentic sample prepared by the reaction of compound **1** with 2-butyne.[9] Isomer **7b** was identified by the close similarity of its spectral parameters with **7a**.

Low-Temperature Reactions. In a typical experiment, in which allene, methylallene, and 1,1-dimethylallene were reacted with compound **1**, 1−3 equiv of the gaseous olefin was added slowly by means of a gastight syringe to a solution of 30 mg (0.02 mmol) of **1** in 0.7 mL of CD_2Cl_2 in an NMR tube cooled to −78 °C in a solid CO_2/acetone bath. One-dimensional NMR spectra (^1H, ^{31}P) were recorded from −80 °C to ambient temperature at 10 °C intervals. As discussed in the Results section, two-dimensional NMR studies (^1H-COSY, TOCSY, ROESY, and $^{13}C{-}^1H$ HMQC) were carried out for any new compounds observed at the appropriate temperatures. The results of these studies are summarized in Table 1. The details of these low-temperature reactions are given below for each cumulene studied.

(g) Allene. Addition of allene to a red solution of **1** at −78 °C resulted in a color change to yellow. Monitoring the ^1H and ^{31}P NMR spectra at −80 °C showed the presence of two major species, **2a** and **2b**, along with minor amounts of unidentified products and approximately 5% of a third isomer, **2c**. Warming the sample resulted in an increase in the amount of **2c** at the expense of **2a** and **2b**, which disappeared together. By −30 °C **2c** was the only significant product observed, although small amounts of new species **2d** and **2e** were becoming evident. Upon further warming, **2c** disappeared while **2d** and **2e** increased, such that by 0 °C all three were present in comparable proportions. By 10 °C only **2d** and **2e** remained, and maintaining this temperature for 1−2 h resulted in the disappearance of **2d**, leaving only **2e**. Spectral parameters for **2a** and **2b** were obtained at −80 °C, those for **2c** were obtained at −30 °C, and those for **2d** were obtained at 10 °C.

(h) Methylallene. Addition of methylallene at −78 °C followed by immediate monitoring of the ^{31}P NMR spectrum at −80 °C showed the presence of **3a** and **3b** in a 1:1 ratio together with trace amounts of **3c**. Varying amounts of **3c** could be observed depending upon our level of success at maintaining the temperature at −78 °C during cumulene addition. Warming resulted in a disappearance of **3a** and **3b** while the concentration of **3c** increased. By −40 °C **3c** was the only species present. Raising the temperature resulted in the appearance of **3d** and **3e**. By 0 °C **3c** has disappeared, leaving only **3d** and **3e**, and by 20 °C **3d** had disappeared, leaving only **3e**. The NMR spectral parameters for **3a** and **3b** were obtained at −80 °C, those for **3c** were obtained at −40 °C, those for **3d** at −10 °C, and those for **3e** at ambient temperature.

(i) 1,1-Dimethylallene. Addition of 1,1-dimethylallene at −78 °C and immediate monitoring by ^{31}P NMR at −80 °C showed **4a** as the only product. Warming the sample resulted in the appearance of **4d** at approximately −20 °C, and by 20 °C this was the only product. No additional species were observed.

(j) 1,1-Difluoroallene. In a typical experiment 0.5−2.0 equiv of 1,1-difluoroallene, generated as described above at −40 °C, was passed into the solution of 30 mg (0.02 mmol) of **1** in 0.7 mL of CD_2Cl_2 in an NMR tube at −78 °C. Diethyl ether-d_{10} was used as solvent in the generation of the 1,1-difluoroallene so that the ether carried over in the difluoroallene stream did not interfere with the ^1H NMR spectrum. One-dimensional NMR spectra (^1H, ^{13}C, ^{19}F, ^{31}P) were recorded from −80 °C to ambient temperature at 10 °C intervals. As discussed in the Results section, two-dimensional NMR studies (^1H-COSY and ROESY) were carried out at particular temperatures. The results of these studies are summarized in Table 1. At −80 °C, the NMR studies showed the presence of only one product (**5a**), the characterization of which is discussed later. At temperatures above −20 °C compound **5a** was replaced by **5c**. If 1,1-difluoroallene was present in excess, varying amounts of other unidentified products were obtained,

so reactions were best carried out with a slight excess of **1**, leading to some unreacted **1** in the final solution.

Low-Temperature Ligand Exchange. In a typical experiment, 1 mL of gaseous cumulene, delivered via a gastight syringe, was reacted with 30 mg of compound **1** in 0.7 mL of CD_2Cl_2 in an NMR tube that had been cooled to −78 °C. The reaction was taken to completion at this temperature, ensuring that no compound **1** remained, as established by $^{31}P\{^1H\}$ and ^1H NMR spectroscopy. At this point, 1 mL of a different cumulene was added by syringe while maintaining the temperature at −78 °C. Upon returning the sample to the spectrometer at −80 °C, monitoring was continued while raising the temperature in 20 °C intervals.

(k) Methylallene Addition to Compounds 2a and 2b. To a mixture of **2a** and **2b** generated at −78 °C as noted above was added 1 mL of methylallene. Monitoring the $^{31}P\{^1H\}$ NMR spectrum at this temperature showed the immediate appearance of small amounts of **3a/3b** together with **2a/2b** as the dominant species. Warming and subsequent mixing led to mixtures of **2c/2d/2e** and **3c/3d/3e** in which the **3**:**2** ratio slowly increased with time. While the proportions of isomers varied throughout the different temperatures, as explained earlier, the final proportions of compounds **2** and **3** were comparable. Leaving the sample at ambient temperature for several hours resulted in the formation of only **2e** and **3e** in comparable proportion.

(l) Allene Addition to Compounds 3a and 3b. To a mixture of **3a** and **3b** at −78 °C was added 1 mL of allene, leading to the immediate appearance of **2a** and **2b** together with **3a** and **3b**. Warming gave rise to mixtures of the isomers of compounds **2** and **3** as described in part (k).

(m) Methylallene Addition to Compound 2c. The isomeric mix of **2a** and **2b** was warmed to −20 °C until the major species present was **2c**. Addition of methylallene at this temperature resulted in the immediate appearance of **3c**, and warming led to mixtures of **2d**, **3d**, **2e**, and **3e**, which after several hours had converted to approximately equal amounts of **2e** and **3e**.

(n) Addition of Allene to Compound 4a. To a solution of **4a**, generated at −78 °C as described above, was added 1 mL of allene. No additional species were observed until the sample was warmed to −60 °C, at which point **2c** began to appear. As the temperature was raised, the proportion of **4a** slowly diminished while that of **2c** increased. At −10 °C **2d** and **2e** began to appear together with **4a**, and raising the temperature to ambient yielded mainly **2e** with small amounts (ca. 10%) of **4d**.

(o) Allene Addition to Compound 5a. Addition of 1 mL of allene to a solution of **5a** at −78 °C, generated as described above, showed no spectroscopic evidence for formation of any product other than **5a**. Upon warming to ambient temperature, only **5a** and **5c** were observed at the appropriate temperatures.

X-ray Data Collection. X-ray quality crystals of **2e** were grown by slow diffusion of diethyl ether into a concentrated 1:1 CH_2Cl_2/toluene solution of the compound. Crystals of **5c** were grown from ether/CH_2Cl_2. Data for **2e** were collected at −60 °C on a Siemens P4/RA SMART 1K CCD diffractometer, while for **5c** data were collected on a Bruker PLATFORM/SMART 1000 CCD diffractometer at −80 °C.[15] Unit cell parameters were obtained from a least-squares refinement of 8192 and 6256 reflections for the respective compounds. For both compounds, the cell parameters and the diffraction symmetry established the space groups as $P1$ or $P\bar{1}$, the latter of which was established as correct by the successful refinement of both structures. Absorption corrections were applied to **2e** by the SADABS method, supplied through the Bruker software, while for **5c** the crystal faces were indexed and measured, with absorption corrections carried out using Gaussian integration. See Table 2 for a summary of X-ray data collection information.

Structure Solution and Refinement. Both structures were solved using the direct methods program SHELXS-86,[16] and refinement was completed using SHELXL-93.[17] Hydrogen atoms were assigned positions based on the geometries of the attached carbon atoms and were assigned thermal parameters 20% greater than those of the attached carbons. For compound **2e** there are two unique molecules per asymmetric unit, although the parameters for both agree very well. In compound **5c**, one of the CH_2Cl_2 molecules of crystallization was disordered over two positions of half occupancy in the unit cell. Further details of structure refinement and final residual indices are found in Table 2.

Results and Compound Characterization

(a) Cumulene Adducts. The binuclear methyl complex $[Ir_2(CH_3)(CO)(\mu\text{-}CO)(dppm)_2][CF_3SO_3]$ (**1**) reacts readily with allene, methylallene, 1,1-dimethylallene, and 1,1-difluoroallene at −78 °C, but upon warming, the initial products undergo a number of subsequent rearrangements. Each of the intermediates in these transformations has been characterized at the appropriate temperature by NMR techniques, while species that could be isolated have also been characterized by additional methods, as is described in what follows.

(i) Allene. At −78 °C the reaction of **1** with allene yields two products (**2a** and **2b**) in approximately equal proportions as outlined in Scheme 2. The $^{31}P\{^1H\}$ NMR spectrum of this mixture shows three resonances at δ −9.0, −6.7, and −1.6, in an approximate 1:1:2 intensity ratio. Whereas the two high-field signals each appear as one-half of an AA′BB′ pattern from two separate species, the low-field signal of double intensity is complex and corresponds to two coincidentally overlapping signals from the other halves of the above patterns. The ^1H NMR spectrum at this stage of the reaction is complicated owing to the overlapping, broad resonances of both species. Nevertheless, two broad signals are identified at δ −12.25 and 4.99, corresponding to hydride and methylene groups, respectively. Although selective ^{31}P decoupling experiments fail to give useful resolution of the overlapping methylene signals, these experiments clearly resolve two different, but closely spaced hydride resonances (δ −12.20, −12.30) for **2a** and **2b**. The $^{13}C\{^1H\}$ NMR spectrum of a ^{13}CO-enriched sample shows four resonances of comparable intensity at δ 190.3, 189.3, 176.1, and 174.8, consistent with the presence of two dicarbonyl complexes. We were unable to identify which pairs of carbonyl resonances belonged together, although we assume that the spectrum for each compound is very similar, giving rise to one high- and one low-field resonance in each case; certainly, the two high-field signals are very close, as are the two low-field ones.

The presence of methylene and hydride fragments in these products is reminiscent of our previous work in which ligand addition to one metal in **1** resulted in C−H bond cleavage of the methyl ligand by the adjacent metal, as diagrammed in Scheme 1.[4d,6] We therefore propose that addition of allene has resulted in a similar C−H activation process yielding two isomers, $[Ir_2(H)$-

(15) Programs for diffractometer operation, data reduction, and absorption correction were those supplied by Bruker or Siemens.

(16) Sheldrick, G. M. *Acta Crystallogr.* **1990**, *A46*, 467.
(17) Sheldrick, G. M. *SHELXL-93*, Program for structure determination; University of Göttingen: Germany, 1993.

Table 2. Crystallographic Data for Compounds 2e and 5c

	$[Ir_2(CH_3)(CO)_2(\mu\text{-}\eta^1{:}\eta^3\text{-}H_2C{=}C{=}CH_2)(dppm)_2][CF_3SO_3]$ (**2e**)·1/3CH_2Cl_2	$[Ir_2(CH_3(CO)(\mu\text{-}H_2C{=}C{=}CF_2)(dppm)_2][CF_3SO_3]$(**5c**)·2$CH_2Cl_2$
A. Crystal Data		
formula	$C_{57.33}H_{51.67}Cl_{0.67}F_3Ir_2O_5P_4S$	$C_{59}H_{53}Cl_4F_5Ir_2O_5P_4S$
fw	1441.65	1619.15
cryst dimens (mm)	0.24 × 0.14 × 0.03	0.26 × 0.24 × 0.10
color	yellow	orange
cryst syst	triclinic	triclinic
space group	$P\bar{1}$ (No. 2)	$P\bar{1}$ (No. 2)
unit cell params[a,b]		
a (Å)	10.4603(1)	12.327(1)
b (Å)	14.2406(1)	17.297(2)
c (Å)	38.7838(4)	17.821(2)
α (deg)	91.887(1)	63.059(2)
β (deg)	97.732(1)	76.554(2)
γ (deg)	90.281(1)	70.189(2)
V (Å^3)	5721.39(9)	3172.8(6)
Z	4	2
ρ_{cacd} (g cm^{-3})	1.674	1.695
μ (mm^{-1})	4.882	4.552
B. Data Collection and Refinement Conditions		
diffractometer	Siemens P4/RA/SMART 1K CCD[c]	Bruker PLATFORM/SMART 1000 CCD[d]
radiation (λ [Å])	graphite-monochromated Mo Kα (0.71073)	
temp (°C)	−60	−80
scan type	ϕ rotations (0.3°) and ω scans (0.3°) (10 s exposures)	ω scans (0.2°) (25 s exposures)
data collection 2θ limit (deg)	55.00	52.90
total data collected	63 233 ($-13 \le h \le 13$, $-18 \le k \le 18$, $-50 \le l \le 50$)	17 665 ($-15 \le h \le 15$, $-19 \le k \le 21$, $-22 \le l \le 21$)
no. of indep reflns	23 466 (R_{int} = 0.1958)	12 736 (R_{int} = 0.0416)
no. of obsd refns (NO)	10 928 ($F_o^2 \ge 2\sigma(F_o^2)$)	8785 ($F_o^2 \ge 2\sigma(F_o^2)$)
range of transm factors	0.6468−0.4616	0.6589−0.3840
no. of data/restraints/params	23466 [$F_o^2 \ge -3\sigma(F_o^2)$]/0/1312	12 736[$F_o^2 \ge -3\sigma(F_o^2)$] / 0/748
extinction coeff (χ)[e]	0.00027(3)	
largest diff peak and hole (e Å^{-3})	1.521 and −1.149	4.735 and −2.150
final R indices[f]		
R_1 ($F_o^2 \ge 2\sigma(F_o^2)$)	0.0867	0.0549
wR_2 ($F_o^2 \ge -3\sigma(F_o^2)$)	0.1853	0.1447
goodness of fit (S)[g]	1.034	1.026

[a] For **2e**, obtained from least-squares refinement of 8192 centered reflections. [b] For **5b**, obtained from least-squares refinement of 6256 centered reflections. [c] Programs for diffractometer operation, data collection, data reduction, and absorption correction were those supplied by Siemens. [d] Programs for diffractometer operation, data collection, data reduction, and absorption corrections were those supplied by Bruker. [e] $F_c^* = kF_c[1 + x\{0.001F_c^2\lambda^3/\sin(2\theta)\}]^{-1/4}$ where k is the overall scale factor. [f] $R_1 = \Sigma||F_o| - |F_c||/\Sigma|F_o|$; $wR_2 = [\Sigma w(F_o^2 - F_c^2)^2/\Sigma w(F_o^4)]^{1/2}$. [g] $S = [\Sigma w(F_o^2 - F_c^2)^2/(n - p)]^{1/2}$ (n = number of data; p = number of parameters varied; $w = [\sigma^2(F_o^2) + (a_oP)^2 + a_1P]^{-1}$ where $P = [\mathrm{Max}(F_o^2, 0) + 2F_c^2]/3$). For **2e** a_o = 0.0456, a_1 = 22.8603; for **5b** a_o = 0.0766, a_1 = 1.4138.

(η^2-C_3H_4)(CO)$_2$(μ-CH_2)(dppm)$_2$][CF_3SO_3] (**2a**, **2b**), which differ only in the orientation of the η^2-allene fragment with respect to the bridging methylene group. This interpretation is consistent with the very close spectral similarities in these two products, which additionally bear a close resemblance to the ethylene adduct [Ir_2H-(η^2-C_2H_4)(CO)$_2$(μ-CH_2)(dppm)$_2$][CF_3SO_3], reported elsewhere.[4d] Owing to the overlap of most ^{1}H NMR signals of these isomers, appropriate experiments to determine which isomer was which could not be carried out.

Upon warming this sample, an additional species (**2c**), which at −78 °C is barely discernible in the $^{31}P\{^1H\}$ NMR spectrum, grows in intensity at the expense of **2a** and **2b**, and by −30 °C this product accounts for 90% of the integrated intensity. The $^{31}P\{^1H\}$ NMR pattern for **2c** at this temperature is that of an AA′BB′ spin system with resonances at δ 25.3 and −5.5. This new product displays no hydride resonance in the ^{1}H NMR spectrum, and the only methylene signals observed are those corresponding to the dppm ligands (δ 3.62, 3.44) and the allene ligand (vide infra). Instead, this spectrum displays a triplet signal at δ 0.18, corresponding to an iridium-bound methyl group. The allene protons appear in a 1:1:2 intensity ratio, respectively, as two singlets, at δ 6.06 and 4.01 and a triplet displaying coupling to two adjacent ^{31}P nuclei at δ 2.46. To ascertain the bonding mode of the allene ligand, a ^{1}H-ROESY experiment was carried out at −30 °C. NOE contacts were observed between the high-field allene protons and one set of dppm methylene protons (δ 3.62), while one of the protons (δ 4.01) at the other end of the allene ligand showed a contact with the iridium-bound methyl group. The remaining allene proton (δ 6.06) showed a strong NOE with its geminal partner, but with no other proton. These results suggest the bridging arrangement for the allene ligand as shown in Scheme 2, in which one allene proton on the uncoordinated allene double bond is in close proximity to the iridium-bound methyl ligand, while the other is aimed away. The high-field signal that displays ^{31}P coupling clearly corresponds to the allene methylene group that is bound to one metal. These protons lie above and below the Ir_2-allene plane and could come into close contact with one proton on each of the dppm methylene groups. This bridged-allene binding mode has been proposed in the thermally unstable $Os_2(CO)_8(\mu\text{-}\eta^1{:}\eta^1\text{-}H_2C{=}C{=}CH_2)$,[18] and such bridged binding modes are common for alkynes[9,19] and also known for olefins.[4d,20] It is also the coordination

(18) Spetseris, N.; Norton, J. R.; Hunter, D. R. *Organometallics* **1995**, *14*, 603.

Scheme 2

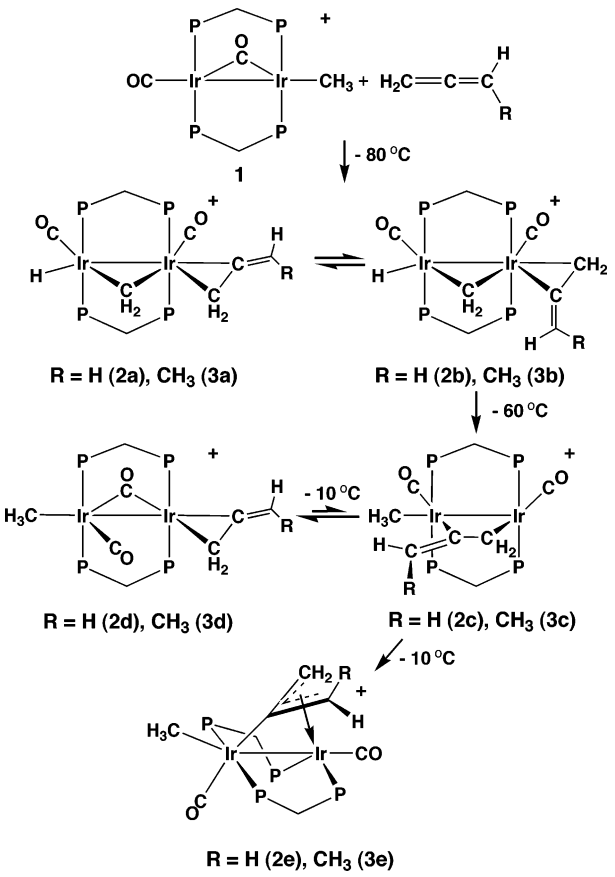

mode observed, apart from the orientation of the cumulene ligand, in the 1,1-difluoroallene adduct $[Ir_2(CH_3)(CO)_2(\mu\text{-}\eta^1{:}\eta^1\text{-}H_2C{=}C{=}CF_2)(dppm)_2][CF_3SO_3]$ (**5c**) (vide infra). In the ^{13}C NMR spectrum of **2c** the expected two carbonyl resonances are observed at δ 192.4 and 186.2, consistent with terminal carbonyl binding.

At approximately −10 °C two additional products, **2d** and **2e**, begin to appear in the $^{31}P\{^1H\}$ NMR spectrum, and their appearance corresponds to the disappearance of the resonance for **2c**. Compound **2d** appears as two resonances at δ 19.5 and 2.5, with patterns typical of an AA′BB′ spin system, while **2e** appears as a single complex multiplet at δ −15.7. At 10 °C compound **2c** has disappeared, and maintaining this temperature results in the disappearance of **2d** over a 2 h period, leaving only **2e**. The ^1H NMR spectrum of **2d** shows a methyl resonance as a triplet at δ 1.23 with coupling to the adjacent pair of ^{31}P nuclei, and three allene resonances at δ 5.61, 4.81, and 4.24 in a 1:1:2 ratio. Two closely spaced carbonyl resonances are observed in the ^{13}C NMR spectrum at δ 206.6 and 206.2. Although these ^{13}C chemical shifts suggest the presence of two semibridging carbonyls having somewhat different environments, we propose, based on analogies with the ethylene adduct $[Ir_2(CH_3)(\eta^2\text{-}C_2H_4)(CO)_2(dppm)_2][CF_3SO_3]$[4d] and with the dimethylallene adduct (**4d**), the characterization of

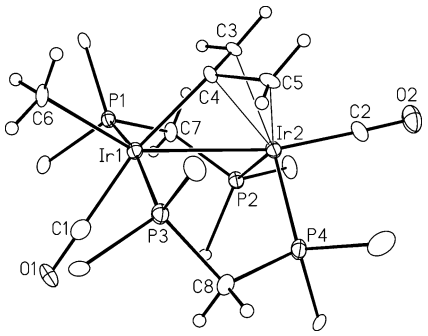

Figure 1. Perspective view of one of the two crystallographically independent $[Ir_2(CH_3)(CO)_2(\mu\text{-}\eta^1{:}\eta^3\text{-}H_2C{=}C{=}CH_2)(dppm)_2]^+$ cations of compound **2e**. Thermal ellipsoids are shown at the 20% probability level except for hydrogens, which are shown artificially small. Only the ipso carbons of the dppm phenyl rings are shown.

which is discussed in detail later in the text, that **2d** has one terminal and one bridging carbonyl, which interchange rapidly on the NMR time scale. An alternate structure in which the positions of the methyl group and the terminal carbonyl are interchanged can be ruled out on the basis that the low-field carbonyl resonances are indicative of carbonyls that lie in the vicinity of an adjacent metal rather than being remote from this metal.[21]

Crystals of compound **2e** were obtained, and an X-ray investigation established the unusual structure of this product, as diagrammed in Figure 1. This fifth isomer, $[Ir_2(CH_3)(CO)_2(\mu\text{-}\eta^1,\eta^3\text{-}C_3H_4)(dppm)_2][CF_3SO_3]$ (**2e**), has the allene ligand η^1 bound via the central carbon to one metal, while being η^3 bound to the second metal. Two crystallographically distinct molecules are present in the asymmetric unit cell, and these are identified as molecules A and B in Table 3. The geometry at Ir(1) is distorted octahedral, in which the two phosphines are mutually *trans*, the carbonyl is essentially opposite the central carbon of the allene moiety, and the methyl ligand is almost opposite the metal−metal bond. At Ir(2) the geometry can also be viewed as distorted octahedral, however with a *cis* arrangement of phosphines in which each phosphorus is opposite the ends of the η^3-allyl unit. At this metal, the carbonyl is opposite the metal−metal bond. The bonding parameters associated with the bridging allene ligand are essentially as expected. The Ir(1)−C(4) distance (2.09(2), 2.10(2)Å for the two molecules) is somewhat shorter than the Ir−CH_3 distance (2.19(2), 2.20(2)Å), a difference that is consistent with the hybridization differences of the bound carbons (sp^2 vs sp^3, respectively), and the distances from Ir(2) to the three allylic carbons (2.12−2.21 Å) are, as expected, longer than the Ir(1)−C(4)) σ bond. Within the bridging allene group, the distances (1.41−1.45 Å) and the C(3)−C(4)−C(5) angle (108(2)°, 106(2)°) are typical of η^3-bound allyl moieties.[22,23] Although not common, similar bridging allene coordination has previously been observed.[24]

In solution the NMR spectral results are consistent with the above geometry being maintained. The ^{13}C-

(19) See for example: (a) Gagné, M. R.; Takats, J. *Organometallics* **1988**, *7*, 561. (b) Dickson, R. S. *Polyhedron* **1991**, *10*, 1995. (c) Adams, R. D.; Huang, M. *Organometallics* **1995**, *14*, 2887. (d) George, D. S. A., McDonald, R.; Cowie, M. *Can. J. Chem.* **1996**, *74*, 2289.

(20) See for example: (a) Grevels, F.-W.; Klotzbücher, W. E.; Siels, F.; Schaffner, K.; Takats, J. *J. Am. Chem. Soc.* **1990**, *112*, 1995. (b) Bender, B. R.; Ramage, D. L.; Norton, J. R.; Wiser, D. C.; Rappé, A. K. *J. Am. Chem. Soc.* **1997**, *119*, 5628.

(21) George, D. S. A.; McDonald, R.; Cowie, M. *Organometallics* **1998**, *17*, 2553.

(22) Hay, C. M. Horton, A. D.; Mays, M. J.; Raithby, P. R. *Polyhedron* **1988**, *7*, 987.

(23) Orpen, A. G.; Brammer, L.; Allen, F. H.; Kennard, O.; Watson, D. G.; Taylor, R. *J. Chem. Soc., Dalton Trans.* **1989**, 51.

Table 3. Selected Distances and Angles for Compound 2e

(a) Distances (Å)

atom 1	atom 2	molecule A distance	molecule B distance
Ir(1)	Ir(2)	2.8438(10)	2.8353(9)
Ir(1)	P(1)	2.365(5)	2.361(5)
Ir(1)	P(3)	2.371(5)	2.335(5)
Ir(1)	C(1)	1.90(2)	1.91(2)
Ir(1)	C(4)	2.09(2)	2.10(2)
Ir(1)	C(6)	2.19(2)	2.20(2)
Ir(2)	P(2)	2.317(4)	2.341(5)
Ir(2)	P(4)	2.329(5)	2.336(5)
Ir(2)	C(2)	1.88(2)	1.90(2)
Ir(2)	C(3)	2.20(2)	2.21(2)
Ir(2)	C(4)	2.12(2)	2.13(2)
Ir(2)	C(5)	2.21(2)	2.21(2)
O(1)	C(1)	1.13(2)	1.14(2)
O(2)	C(2)	1.17(2)	1.12(2)
C(3)	C(4)	1.41(2)	1.45(2)
C(4)	C(5)	1.44(2)	1.44(2)

(b) Angles (deg)

atom 1	atom 2	atom 3	molecule A angle	molecule B angle
Ir(2)	Ir(1)	C(1)	121.1(5)	117.9(5)
Ir(2)	Ir(1)	C(4)	48.0(4)	48.5(5)
Ir(2)	Ir(1)	C(6)	148.6(4)	151.6(5)
P(1)	Ir(1)	P(3)	167.8(2)	173.1(2)
C(1)	Ir(1)	C(4)	169.1(7)	166.4(7)
C(1)	Ir(1)	C(6)	90.2(7)	90.5(7)
C(4)	Ir(1)	C(6)	100.6(6)	103.1(7)
P(2)	Ir(2)	P(4)	108.5(2)	114.5(2)
Ir(1)	C(1)	O(1)	180(1)	178(2)
Ir(2)	C(2)	O(2)	179(2)	176(2)
Ir(2)	C(3)	C(4)	68(1)	67.6(9)
Ir(1)	C(4)	Ir(2)	84.9(5)	84.1(5)
Ir(1)	C(4)	C(3)	119(1)	121(1)
Ir(1)	C(4)	C(5)	120(1)	119(1)
Ir(2)	C(4)	C(3)	74.1(9)	74(1)
Ir(2)	C(4)	C(5)	73.8(9)	73(1)
C(3)	C(4)	C(5)	108(2)	106(2)
Ir(2)	C(5)	C(4)	67.5(8)	68(1)

{^{1}H} NMR spectrum displays resonances at δ 179.2 and 171.2 for the terminal carbonyls, a multiplet at δ 61.3 for the terminal carbons of the allene group, and a triplet at δ −31.1 for the methyl ligand. An INEPT experiment shows the central allene carbon as a multiplet at δ 127.3, which is typical for the central carbon of η^3-allyl groups.[25] The ^{1}H NMR spectrum shows signals for the allene protons at δ 4.23 and 3.52 arising from the *anti* and *syn* protons, respectively, as established by NOE experiments. An HMQC experiment shows that both of these signals arise from protons on two carbons that are chemically equivalent. The resonance for the Ir-bound methyl group appears as a triplet at δ 1.18 showing 5 Hz coupling to two adjacent phosphorus nuclei. Although the structure established for **2e** would be expected to give rise to two resonances in the ^{31}P{^{1}H} NMR spectrum, corresponding to the two chemically inequivalent ends of the dppm ligands, only one complex multiplet is observed, resulting from accidental overlap of the two expected signals.

(ii) Methylallene. The reaction of **1** with methylallene very much parallels that of allene, as described above. At −78 °C the reaction mixture contains two major products in approximately equal proportions, as shown by the ^{31}P{^{1}H} NMR spectrum, together with a third minor species. The two major species, **3a** and **3b**, having ^{31}P{^{1}H} resonances at δ −0.4 and −6.9 and at δ −2.6 and −8.0 are also hydrides, with resonances in the ^{1}H NMR spectrum at δ −12.0 and −12.6, respectively. Unfortunately, additional features could not be established from the ^{1}H NMR spectrum owing to overlap, particularly in the methylene region. However, each species **3a** and **3b** also displays a pair of resonances in the ^{13}C NMR spectrum at approximately δ 190 and 176, corresponding to terminal carbonyls. The close spectral similarities of these products and their resemblance to **2a** and **2b** suggest the isomers shown in Scheme 2, having the formulation [$Ir_2H(\eta^2$-$H_2C{=}C{=}C(H)Me)(CO)_2$-(μ-CH_2)(dppm)$_2$][CF_3SO_3], in which η^2 coordination of methylallene at one metal has resulted in C−H activation of the methyl ligand at the adjacent metal. Again, we were unable to determine which isomer corresponds to which set of NMR resonances.

As the temperature is raised, the proportion of the minor component (**3c**) increases at the expense of both **3a** and **3b**, and between −40 and −20 °C compound **3c** is the predominant species. In the ^{1}H NMR spectrum at −40 °C, compound **3c** gives rise to a triplet corresponding to an Ir-bound methyl ligand at δ 0.23 ($^3J_{PH}$ = 6.6 Hz) and the dppm methylenes at δ 3.45. In this spectrum resonances for the methylallene ligand appear at δ 1.76, 3.80, and 2.07 in a 3:1:2 ratio, corresponding to the methyl substituent, the adjacent unique hydrogen, and the geminal CH_2 protons, respectively. The resonance corresponding to the CH_2 moiety appears as a triplet which collapses to a singlet when the low-field ^{31}P resonance is irradiated. Decoupling the high-field ^{31}P resonance results in collapse of the resonance for the methyl ligand to a singlet and at the same time results in sharpening of the ^{1}H signals at δ 1.76 and 3.80. These selective ^{31}P-decoupling experiments establish that the methylallene ligand in **3c** bridges the metals, much as proposed for the allene-bridged **2c**. Support for this formulation was obtained by a ROESY experiment in which NOE was observed between the unique hydrogen of methylallene and the Ir-bound methyl group but *not* between the two methyl groups. NOE was also observed between the geminal CH_2 protons of the methylallene ligand and one pair of dppm methylene protons.

At temperatures above −20 °C two new species (**3d** and **3e**) begin to appear at approximately the same rate until **3c** disappears, after which **3d** slowly disappears, leaving only **3e**, which increases by a corresponding amount. Although many of the ^{1}H resonances of **3d** overlap with those of **3e**, the other spectral parameters allow us to identify this intermediate with some confidence. An iridium-bound methyl resonance appears as a triplet at δ 1.25 in the ^{1}H NMR spectrum, and no

(24) (a) Davis, R. E. *Chem. Commun.* **1968**, 248. (b) Kühn, A.; Burschka, Ch.; Werner, H. *Organometallics* **1982**, *1*, 496. (c) Arce, A. J.; DeSanctis, Y.; Deeming, A. J.; Hardcastle, K. I.; Lee, R. *J. Organomet. Chem.* **1991**, *406*, 209. (d) Chetcuti, M. J.; Fanwick, P. E.; McDonald, S. R.; Roth, N. N. *Organometallics* **1991**, *10*, 1551. (e) Chacon, S. T.; Chisholm, M. H.; Folting, K.; Huffman, J. C.; Hampden-Smith, M. J. *Organometallics* **1991**, *10*, 3722. (f) Seyferth, D.; Anderson, L. L.; Davis, W. B.; Cowie, M. *Organometallics* **1992**, *11*, 3736. (g) Chisholm, M. H.; Folting, K.; Lynn, M. A.; Streib, W. E.; Tiedtke, D. B. *Angew. Chem., Int. Ed. Engl.* **1997**, *36*, 52. (h) Chisholm, M. H.; Streib, W. E.; Tiedtke, D. B.; Wu, D.-D. *Chem. Eur. J.* **1998**, *4*, 1470.

(25) Chu, C. S.; Shin, S. Y.; Lee, C. *J. Chem. Soc., Dalton Trans.* **1992**, 1323.

hydride resonance is observed. In addition, the methyl group of the methylallene ligand appears as a doublet at δ 0.90 (presumably coupled to the hydrogen geminal to it, although this resonance could not be observed to confirm this assignment), shifted upfield from that observed in **3c** (δ 1.76), and the $^{13}C\{^1H\}$ NMR spectrum shows a pair of carbonyls at δ 208.2 and 207.3. As noted earlier for **2d**, we propose a fluxional process that rapidly interconverts the bridging and terminal carbonyls of **3d**. We did not acquire IR data for this intermediate to confirm this assignment; however this has been done for the closely comparable ethylene[4d] and 1,1-dimethylallene (**4d**) adducts. Taken together, these data suggest a structure analogous to these other olefin adducts, in which the methylallene ligand is bound to one metal opposite the Ir−Ir bond from the methyl ligand.

The spectral parameters for **3e** are consistent with the structure shown for $[Ir_2(CH_3)(CO)_2(\mu\text{-}\eta^1{:}\eta^3\text{-}CH_2CCH(Me))(dppm)_2][CF_3SO_3]$ in Scheme 2. Although the average ^{31}P chemical shift for the diphosphine ligands is closely comparable to that of **2e**, the spectrum for **3e** is more complex in keeping with the ABCD spin system that results from the lower symmetry of the complex by virtue of the methyl substituent on one end of the bridging cumulene ligand. Three complex ^{31}P signals appear in a 1:2:1 intensity ratio centered at δ −14.2, −16.2, and −17.5; the two accidentally equivalent ^{31}P nuclei are presumably those adjacent to the methyl ligand, remote from the inequivalent ends of the methylallene ligand. The loss of mirror symmetry bisecting the methylallene ligand upon substitution by the methyl group gives rise to four dppm methylene signals in the ^1H NMR spectrum (δ 5.79, 5.38, 5.19, and 4.87). In this spectrum the pair of geminal protons of the methylallene ligand appear as multiplets at δ 5.17 and 3.78, while the unique ligand proton appears as a quartet of multiplets at δ 4.70. The allene methyl group appears as a pseudo triplet ($^3J_{HH}$ = 6 Hz, $^4J_{PH}$ = 6 Hz) at δ 1.07, showing coupling to its adjacent hydrogen and to one phosphorus nucleus (presumably the one that is in a pseudo-*trans* position), and the Ir-bound methyl appears as the usual triplet at δ 1.16. In the $^{13}C\{^1H\}$ NMR spectrum (natural abundance) the pair of terminal allene carbons appear as multiplets at δ 78.7 and 55.6, the allene methyl group appears as a multiplet at δ 18.6, and the Ir-bound methyl appears as a triplet at δ −32.2. The location of the allylic methyl group in the endo site, as diagrammed in Scheme 2, was confirmed by NOE experiments in which NOE contacts were detected between this methyl group and both the hydrogen geminal to it and one of the hydrogens on the other end of the allyl unit. NOE contacts between the pair of geminal hydrogens were also observed.

(iii) 1,1-Dimethylallene. The reaction of **1** with 1,1-dimethylallene at −78 °C yields only one product, $[Ir_2H(\eta^2\text{-}CH_2{=}C{=}CMe_2)(CO)_2(\mu\text{-}CH_2)(dppm)_2][CF_3SO_3]$ (**4a**), exactly analogous to the initial products in the low-temperature reactions of **1** with ethylene, allene, and methylallene. The $^{31}P\{^1H\}$ NMR spectrum displays two resonances at δ 1.3 and −13.7, having the classic pattern for an AA′BB′ spin system in these dppm-bridged complexes, while the $^{13}C\{^1H\}$ NMR spectrum of a ^{13}CO-enriched sample shows two terminal-carbonyl

Scheme 3

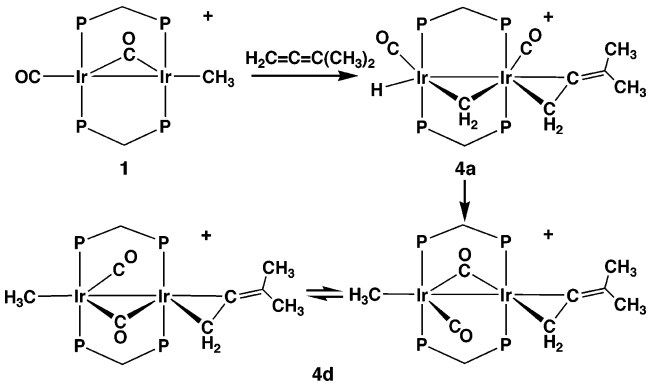

resonances at δ 191.1 and 178.2. Compound **4a** is unambiguously identified as a methylene hydride species, as shown in Scheme 3, by the hydride resonance at δ −12.1 and the methylene resonance at δ 5.96 in the ^1H NMR spectrum. In this spectrum the dppm methylene protons appear as their usual pattern at δ 5.16 and 3.48, while the methylene protons of the cumulene ligand appear as a signal at δ 1.90. Two distinct signals appear for the two methyl substituents of the cumulene at δ 1.13 and 0.19. The appearance of only one CH_2 resonance and two methyl signals indicates that the dimethylallene ligand is bound to the metal by the less sterically encumbered end, since in such a binding mode the $=CH_2$ protons are chemically equivalent, lying above and below the cumulene plane, while the *syn*- and *anti*-methyl groups are inequivalent.

Warming a CH_2Cl_2 solution of **4a** results in a transformation to $[Ir_2(CH_3)(\eta^2\text{-}CH_2{=}C{=}CMe_2)(CO)_2(dppm)_2][CF_3SO_3]$ (**4d**) with no other species being observed. This product is analogous to the ethylene adduct previously described[4d] and to compounds **2d** and **3d**. The spectral parameters of these species are closely comparable. In the ^1H NMR spectrum the dppm methylene protons appear at δ 3.48 and 3.19, the geminal protons and the two methyl groups of the cumulene appear as a singlet at δ 1.58 and as broad singlets at δ 1.22 and 0.98, respectively, and the Ir-bound methyl group appears as a triplet at δ 1.17. The appearance of one signal for the pair of geminal protons and two signals for the methyl groups again indicates that the dimethylallene group is bound through the less sterically encumbered "$H_2C{=}C$" end of the molecule. Two signals (broad triplets) are seen for the carbonyls at δ 206.4 and 204.8, and selective decoupling suggests that they appear to be primarily bound to the same metal as the methyl ligand, while also interacting weakly with the adjacent metal. However, the IR spectrum, which displays carbonyl stretches at 1793 and 1963 cm^{-1}, suggests a slightly different interpretation in which these carbonyls exchange rapidly between terminal and bridging sites as diagrammed in Scheme 3. Facile exchange of the carbonyls from terminal to bridging gives average resonances in the $^{13}C\{^1H\}$ NMR spectra that appear as a pair of semibridging groups, the environments of which differ slightly owing to the orientation of the cumulene ligand. This fluxionality is analogous to that proposed for the analogous ethylene,[4d] allene (**2d**), and methylallene (**3d**) adducts and is rapid on the NMR time scale, even at −80 °C, but resolvable on the much faster IR time scale.

Scheme 4

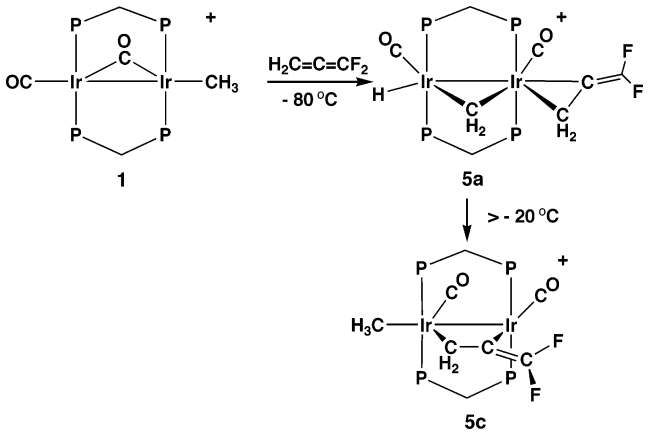

(iv) 1,1-Difluoroallene. As with all other allenes in this study, 1,1-difluoroallene reacts with **1** at −78 °C to yield a methylene-bridged hydride product, $[Ir_2H(\eta^2\text{-}H_2C{=}C{=}CF_2)(CO)_2(\mu\text{-}CH_2)(dppm)_2][CF_3SO_3]$ (**5a**), as diagrammed in Scheme 4. The hydride resonance in the ^1H NMR spectrum appears as a broad signal at δ −12.5, while the bridging methylene and the allene proton resonances (also broad) appear at δ 5.22 and 1.62, respectively. In the $^{13}C\{^1H\}$ NMR spectrum the carbonyl resonances at δ 187.4 and 174.4 are typical for terminally bound groups. The ^{19}F NMR spectrum displays the inequivalent fluoroallene resonances as doublets at δ −80.5 and −97.5, with a mutual geminal coupling of 84 Hz. The triflate resonance appears as a singlet at δ −79.2. As was the case for 1,1-dimethylallene, but unlike those for allene and methylallene, no other isomer for the η^2-bound cumulene adduct is observed at this temperature.

Warming **5a** above −20 °C results in conversion to $[Ir_2(CH_3)(CO)_2(\mu\text{-}H_2C{=}C{=}CF_2)(dppm)_2][CF_3SO_3]$ (**5c**), and by −10 °C this is the only product remaining. If **5a** is prepared in the presence of excess difluoroallene, warming results in the appearance of other unidentified products. To prepare **5c** without these additional products, less than 1 equiv of the allene was used, leaving some unreacted **1** obvious in the NMR spectra.

The ^1H NMR spectrum of **5c** at 27 °C shows, in addition to the dppm resonances, the methyl signal at δ 0.10 as a triplet, having 8.6 Hz coupling to a pair of ^{31}P nuclei, and the allene methylene signal at δ 2.51, also as a triplet ($^3J_{PH}$ = 12.0 Hz). Selective ^{31}P decoupling experiments establish that both CH_3 and CH_2 resonances couple to the same pair of ^{31}P nuclei, so these groups are presumably bound to the same metal. The carbonyl ligands appear at δ 192.4 and 183.0 in the $^{13}C\{^1H\}$ NMR spectrum, while the pair of fluorine resonances in the ^{19}F NMR spectrum appear as doublets at δ −66.9 and −81.6 with mutual coupling of 56 Hz, again consistent with the difluoroallene being bound through the "$H_2C{=}C$" moiety. Overall, the ^{31}P, ^{13}C, and ^1H spectroscopic parameters are similar to those of **2c** and **3c**, suggesting a bridging arrangement for the difluoroallene group as diagrammed in Scheme 4. However, unlike the allene- and methylallene-bridged intermediates, **5c** does not rearrange further upon warming.

The difluoroallene-bridged formulation is confirmed by an X-ray structure determination, and a representation of the compound is shown in Figure 2, with selected bond lengths and angles given in Table 4. Compound **5c** has the normal dppm-bridged arrangement in which the bridging dppm groups are essentially *trans* on both metals. The difluoroallene moiety bridges the metals, as proposed above, through the "$H_2C{=}C$" moiety, having the difluoromethylene moiety as a pendent group. It is noteworthy that the orientation of the bridging cumulene group in **5c** is reversed from that proposed in **2c** and **3c**, having the pendent vinyl group oriented away from the methyl ligand at the adjacent metal and instead pointed toward the less crowded end of the complex, adjacent to the vacant site on Ir(2). We earlier noted that for compounds **2c** and **3c** NOE contacts were observed in the appropriate ^1H NMR spectra between the "$H_2C{=}C$" moiety of the bridging cumulene and one pair of dppm methylene protons. Figure 2 clearly shows close contacts of this type involving the protons on C(3) and the equatorial protons of the dppm methylene groups. These contacts (ca. 2.24 Å) are normal van der Waals separations and clearly short enough to give rise to the observed NOE effects.

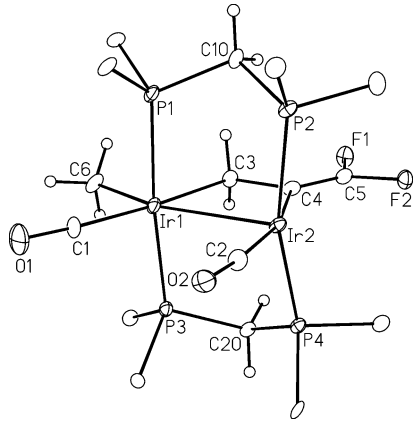

Figure 2. Perspective view of the $[Ir_2(CH_3)(CO)_2(\mu\text{-}\eta^1{:}\eta^1\text{-}CH_2{=}C{=}CF_2)(dppm)_2]^+$ cation of compound **5c**. Thermal ellipsoids as for Figure 1. Only the ipso phenyl carbons are shown.

At Ir(1), which has roughly an octahedral environment, one carbonyl lies almost opposite the methylene group of the bridging allene group, while the methyl ligand is bound almost opposite the Ir−Ir bond. At the other metal the carbonyl lies opposite the other end of the allene bridge. The Ir−Ir separation (2.8844(5) Å) corresponds to a normal single bond and can be viewed as resulting from donation of the d_{z^2} pair of electrons on the square-planar center of Ir(2) to Ir(1), giving the latter an octahedral geometry. In this bonding description the metals are in the +1 and +3 oxidation states, respectively.

The bridging difluoroallene group is essentially symmetrically bound to both metals, having comparable Ir−C distances (2.120(8), 2.110(8) Å), both of which are somewhat shorter than the Ir−CH_3 distance (2.14(1) Å). Binding of the "$H_2C{=}C$" moiety between the metals has resulted in substantial lengthening of the C(3)−C(4) bond to 1.50(1) Å, consistent with a single bond,[25] while at the unbound end the C(4)−C(5) distance (1.31(1) Å) remains as a double bond.

(b) Vinyl Carbene Products. Over a 7-day period at ambient temperature compound **2e** rearranges to the vinyl carbene-bridged product $[Ir_2(H)(CO)_2(\mu\text{-}\eta^1{:}\eta^3\text{-}HCC\text{-}$

Table 4. Selected Interatomic Distances and Angles for Compound 5c

(a) Distances (Å)

atom 1	atom 2	distance	atom 1	atom 2	distance
Ir(1)	Ir(2)	2.8844(5)	Ir(2)	C(4)	2.110(8)
Ir(1)	P(1)	2.342(3)	P(1)	P(2)	3.002(4)[a]
Ir(1)	P(3)	2.343(2)	P(3)	P(4)	2.986(3)[a]
Ir(1)	C(1)	1.894(9)	O(1)	C(1)	1.14(1)
Ir(1)	C(3)	2.120(8)	O(2)	C(2)	1.16(1)
Ir(1)	C(6)	2.14(1)	F(1)	C(5)	1.35(1)
Ir(1)	P(2)	2.314(3)	F(2)	C(5)	1.34(1)
Ir(2)	P(4)	2.335(2)	C(3)	C(4)	1.50(1)
Ir(2)	C(2)	1.867(8)	C(4)	C(5)	1.31(1)

(b) Angles (deg)

atom 1	atom 2	atom 3	angle	atom 1	atom 2	atom 3	angle
Ir(2)	Ir(1)	C(1)	114.3(3)	C(2)	Ir(2)	C(4)	164.5(4)
Ir(2)	Ir(1)	C(3)	71.8(2)	Ir(1)	C(1)	O(1)	171(1)
Ir(2)	Ir(1)	C(6)	159.5(3)	Ir(2)	C(2)	O(2)	173.5(8)
P(1)	Ir(1)	P(3)	173.77(8)	Ir(1)	C(3)	C(4)	107.0(6)
C(1)	Ir(1)	C(3)	173.8(4)	Ir(2)	C(4)	C(3)	111.1(6)
C(1)	Ir(1)	C(6)	86.2(5)	Ir(2)	C(4)	C(5)	129.0(7)
C(3)	Ir(1)	C(6)	87.7(4)	C(3)	C(4)	C(5)	119.9(8)
Ir(1)	Ir(2)	C(2)	94.5(3)	F(1)	C(5)	F(2)	106.8(7)
Ir(1)	Ir(2)	C(4)	70.1(3)	F(1)	C(5)	C(4)	124.5(8)
P(2)	Ir(2)	P(4)	160.86(8)	F(2)	C(5)	C(4)	128.6(8)

[a] Nonbonded distance.

Scheme 5

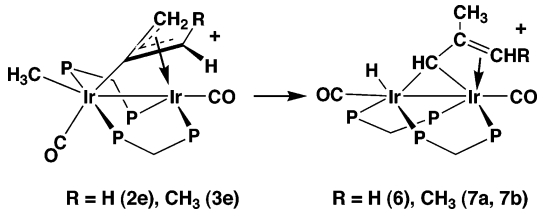

R = H (2e), CH_3 (3e) R = H (6), CH_3 (7a, 7b)

$(CH_3)CH_2)(dppm)_2][CF_3SO_3]$ (**6**), as diagrammed in Scheme 5. Although the yield of **6** is highly variable, it has been obtained in up to approximately 80% yield as determined from $^{31}P\{^1H\}$ NMR spectroscopy. Only minor amounts of other related unidentified species, along with decomposition products which remain at the end, were observed by $^{31}P\{^1H\}$ NMR at intermediate times. The spectroscopy of this product closely resembles that of a series of complexes previously obtained in the reaction of **1** with a number of internal alkynes,[8,9] so we propose an analogous structure for **6**. The structure of one of these products, from the reaction of **1** with 3-hexyne, was previously established by X-ray crystallography.[8,9] The $^{31}P\{^1H\}$ NMR spectrum of **6** is consistent with the structure proposed, appearing as an ABCD spin system in which three resonances in a 2:1:1 intensity ratio appear at δ −5.1, −30.2, and −32.4; the low-field signal of double intensity results from the accidental overlap of two resonances. In the ^1H NMR spectrum the single proton on the bridging alkylidene carbon appears as a broad, unresolved resonance at typically low field (δ 8.72),[9] while the olefinic protons are also broad and appear at δ 3.43 and 3.11. The methyl protons of the vinylcarbene ligand appear as a doublet at δ 2.89, and a hydride signal appears as a multiplet at δ −11.38.

To establish the fate of the Ir-bound methyl group of **2e**, the reaction of allene with $^{13}CH_3$-enriched compound **1** was repeated at ambient temperature. The $^{13}C\{^1H\}$ NMR spectrum of the product showed ^{13}C incorporation into only the 2-methyl site of the vinyl carbene group. With time, compound **6** decomposes into several unidentified species, and it appears that at the same time ^{13}C label becomes scrambled through different sites in what remains of **6**. We have no explanation of this apparent subsequent scrambling.

Compound **3e** also transforms over a several-day period to two isomers of $[Ir_2H(CO)_2(\mu\text{-}\eta^1\text{:}\eta^3\text{-}CHC(CH_3)C(H)CH_3)(dppm)_2][CF_3SO_3]$ (**7a**, **7b**) as the major products together with starting material and minor amounts of several unidentified species. Isomer **7a** was unambiguously identified on the basis of a comparison of its $^{31}P\{^1H\}$ and ^1H NMR spectra with that of a sample previously prepared from the reaction of **1** with 2-butyne.[9] In this isomer the two methyl substituents are mutually *cis*, as confirmed by 2D ^1H NMR experiments in which NOE contacts are established between the two methyl signals at δ 2.72 and 1.42. Isomer **7b** is assumed to have a *trans* arrangement of methyl groups. The isomeric relationship between **7a** and **7b** seems clear on the basis that most ^1H NMR signals for the two species overlap; only the proton on the bridging alkylidene carbon, at δ 8.96, and the hydride signal at δ −11.18 are resolvable from the signals for **7a** (δ 8.79, −11.25). In addition the $^{31}P\{^1H\}$ NMR spectrum for **7b** is closely comparable with that of **7a**.

Discussion

In an earlier study we reported that the methyl complex $[Ir_2(CH_3)(CO)(\mu\text{-}CO)(dppm)_2][CF_3SO_3]$ (**1**) reacted with a variety of ligands, resulting in C−H activation of the methyl ligand to yield methylene-bridged hydrido products, $[Ir_2H(L)(CO)_2(\mu\text{-}CH_2)(dppm)_2][CF_3SO_3]$, in which the added ligand is adjacent to the bridging methylene group.[6] This observation prompted us to attempt analogous reactions using unsaturated organic substrates with the goal of effecting C−C bond formation, by insertion of these substrates into an Ir−CH_2 bond. In the current study we find that cumulenes react with **1**, even at −78 °C, to give the targeted

Scheme 6

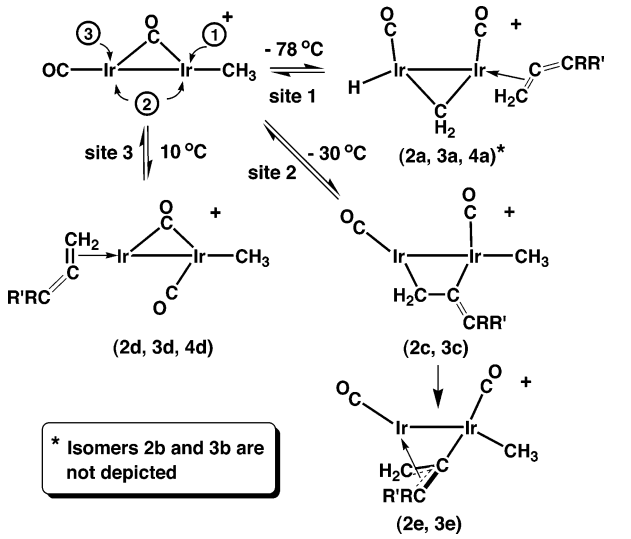

methylene hydride products, analogous to those referred to above (with L = η^2-cumulene). However, for the cumulenes investigated (allene, methylallene, 1,1-dimethylallene, and 1,1-difluoroallene), no subsequent insertion into an Ir−CH_2 bond is observed. Instead, a series of rearrangements, in which the cumulene ligand appears to migrate over the bimetallic framework, is observed. Differences in reactivity of the different cumulenes, as the temperature is increased, can be attributed to either steric or electronic factors associated with the cumulenes, as will be discussed in what follows.

As has been previously discussed,[4d] ligand attack in **1** can occur at one of the three sites shown in Scheme 6 (dppm groups above and below the plane of the drawing are omitted), and several of the isomers observed in this study are consistent with ligand coordination at the different sites being favored at different temperatures. With the four cumulenes studied the kinetic product, observed at −78 °C, results from cumulene attack at site 1, adjacent to the methyl ligand. This is the same site of attack deduced in previous studies for a variety of ligands and results in movement of the methyl ligand toward the adjacent metal at which C−H activation occurs. For allene and methylallene, two isomers are observed for this kinetic product, which differ merely by rotation of the cumulene around the Ir−cumulene bond (only isomer **a** is shown in Scheme 6). There is little preference of one isomer over the other since both isomers for compounds **2** and **3** are present in almost equal proportions. In the case of both disubstituted allenes, only one isomer is observed, presumably owing to unfavorable interactions in the unobserved isomer involving the pair of substituents and the dppm phenyl rings. Although we have no evidence to indicate which isomer is observed, we suggest that both disubstituted allene adducts have geometries like those of **2a** and **3a**, which allow the larger substituents to avoid the bridging methylene group while also presumably minimizing contacts with the phenyl groups. The anticipated insertion of the cumulenes into the adjacent Ir−CH_2 bond does not occur in the low-temperature regime of these products owing presumably to the strong bonds involving the third-row metal.

Warming these products also does not lead to insertion since the aforementioned rearrangements are favored instead. With allene and methylallene, the first rearrangement products observed, at between −60 and −30 °C, are the cumulene-bridged products **2c** and **3c**, respectively. These rearrangements can occur in a couple of ways. In the first case, a partial "merry-go-round" motion of the ligands, in which movement of the cumulene in isomers **2b** or **3b** into the bridging site is accompanied by migration of the hydride ligand back to the methylene group regenerating a methyl ligand, can occur. The second possible pathway involves cumulene dissociation from both isomers **2a**, **2b** or **3a**, **3b**, regenerating **1** followed by cumulene attack at either metal in site 2, with subsequent movement to the bridging position to give **2c** and **3c**, respectively. We favor the latter mechanism, since otherwise it is difficult to rationalize why isomers **2a** and **3a** do not also rotate into a bridging geometry yielding an isomer analogous to the 1,1-difluoroallene adduct, **5c**. Furthermore, this proposal of cumulene dissociation and subsequent recoordination is supported by the formation of mixtures of **2a/2b** together with **3a/3b** when solutions of either **2a/2b** or **3a/3b** are reacted with the *other* cumulene (methylallene or allene, respectively). As described in the Experimental Section, warming such solutions gives rise to all isomers of compounds **2** and **3** at the appropriate temperatures.

In the case of 1,1-difluoroallene, a similar rearrangement occurs, except that the cumulene in this case is coordinated such that the pendent difluorovinyl moiety is adjacent to the metal *remote from the methyl ligand*. Presumably, the alternate geometry, corresponding to isomers **2c** and **3c**, for allene and methylallene, respectively, is unfavorable due to nonbonded contacts between a fluorine substituent and the methyl ligand or due to contacts of these groups with the intervening phenyl groups. In this context, it is worth noting that in the methylallene adduct, **3c**, only the isomer having the allene methyl substituent remote from the methyl ligand, and with the geminal hydrogen aimed toward it instead, is observed. Although the bridged η^1:η^1 binding mode for a cumulene is analogous to that observed for bridged mono-olefin[20] and alkyne-bridged[9,19] complexes, it has apparently never been observed for cumulenes; it has however been proposed as the bonding mode in $Os_2(CO)_8(\mu\text{-}C_3H_4)$.[18] In all other previous reports of cumulene-bridged structures, *both* cumulene π bonds are involved in binding.[24,27] This is believed to be the first unambiguous confirmation of cumulene binding in which a pair of metals bind through only one end of the cumulene, leaving the remaining C=CR_2 moiety as a pendent group.

(26) Allen, F. H.; Kennard, O.; Watson, D. G.; Brammer, L.; Orgpen, A. G.; Taylor, R. *J. Chem. Soc., Perkin Trans. 2* **1987**, 51.
(27) (a) Chisholm, M. H.; Rankel, L. A.; Bailey, W. E., Jr.; Cotton, F. A.; Murillo, C. A. *J. Am. Chem. Soc.* **1977**, *99*, 1261. (b) Bailey, W. I., Jr.; Chisholm, M. H.; Cotton, F. A.; Murillo, C. A.; Rankel, L. A. *J. Am. Chem. Soc.* **1978**, *100*, 802. (c) Lewis, L. N.; Huffman, J. C.; Caulton, K. G. *J. Am. Chem. Soc.* **1980**, *102*, 403. (d) Lewis, L. N.; Huffman, J. C.; Caulton, K. G. *Inorg. Chem.* **1980**, *19*, 1246. (e) Al-Obaidi, Y. N.; Baker, P. K.; Green, M.; White, N. D.; Taylor, G. E. *J. Chem. Soc, Dalton Trans.* **1981**, 2321. (f) Hoel, E. L.; Ansell, G. B.; Leta, S. *Organometallics* **1986**, *5*, 585. (g) Cayton, R. H.; Chisholm, M. H.; Hapden-Smith, M. J. *J. Am. Chem. Soc.* **1988**, *110*, 4438. (h) Cayton, R. H.; Chacon, S. T.; Chisholm, M. H.; Hapden-Smith, M. J.; Huffman, J. C.; Folting, K.; Ellis, P. D.; Huggins, B. A. *Angew Chem., Int. Ed. Engl.* **1989**, *28*, 1523. (i) Wu, I.-Y.; Tseng, T.-W.; Chen. C.-T.; Cheng, M.-C.; Lin, Y.-C.; Wang, Y. *Inorg. Chem.* **1993**, *32*, 1539.

Scheme 7

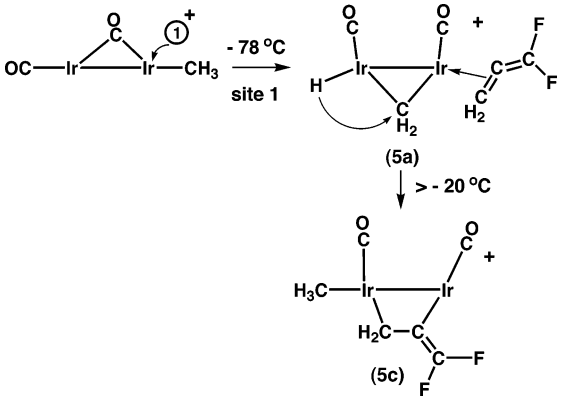

In the case of difluoroallene migration, the transformation of **5a** to **5c** apparently occurs by a merry-go-round movement of the ligands, as outlined in Scheme 7 (dppm groups omitted) instead of by cumulene dissociation and recoordination as described for compounds **2a/2b** and **3a/3b**. Addition of an excess of allene to a solution of **5a** at −78 °C and warming to ambient temperature yields none of the isomers of compound **2**; only **5a** transforming to **5c** is observed. We assume that the electronegative fluorine substituents lead to more effective binding of this cumulene, favoring migration instead of dissociation and recoordination.

It is interesting that in all 1,1-difluoroallene compounds structurally characterized, this group binds preferentially to metals via the hydrogen-substituted double bond.[28] In mononuclear species this has been rationalized in frontier orbital terms as resulting from the LUMO being localized at this end of the molecule, which owing to its strong π-acid nature favors binding to electron-rich metals at this end.[29] In the initial adduct (**5a**) the cumulene binding at one metal through the "$H_2C{=}C$" functionality is presumably favored for the reasons proposed above in mononuclear complexes. The merry-go-round movement of the ligands then generates **5c** which retains binding through the unsubstituted double bond. In any case, the electronegative fluorine substituents clearly favor coordination of the "$H_2C{=}C$" moiety in the bridging position, since subsequent warming does not result in further rearrangement.

Increasing the steric bulk of the substituents even further to the dimethylallene adduct results in no cumulene-bridged isomer being observed; presumably, the steric contacts in such a bridged species are too highly unfavorable. Instead, warming a solution of **4a** results in rearrangement to isomer **4d** (Schemes 3 and 6), which also contains an η^2-bound cumulene bound terminally to one metal. Clearly in this case rearrangement must occur by ligand dissociation since in **4a** the cumulene is flanked by the methylene group and a carbonyl, whereas in **4d** it is flanked by both carbonyls. This has been verified by warming a solution of **4a** in the presence of allene. Although in this case no reaction takes place at −78 °C, warming to −60 °C gives rise to small amounts of **2c** together with **4a**. Further temperature increases result in the increased formation of **2c**

(28) (a) Lentz, D.; Nichelt, N.; Willemsen, S. *Chem. Eur. J.* **2002**, *8*, 1205. (b) Lentz, D. *J. Fluorine Chem.* **2004**, *125*, 853.

(29) Dixon, D. A.; Smart, B. E. *J. Phys. Chem.* **1989**, *93*, 7772.

Scheme 8

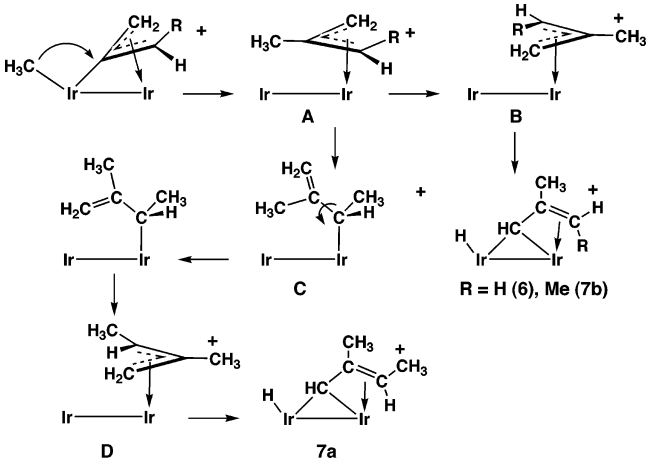

at the expense of **4a**, and at −10 °C **2d** and **2e** also begin to appear. At ambient temperature the major species is **2e** with only minor amounts of **4d** present. Upon dimethylallene dissociation, the smaller allene molecule competes more effectively for the iridium coordination sites.

Warming compound **2c** or **3c** results in two parallel transformations yielding simultaneously the η^2-cumulene adducts **2d** or **3d** together with the $\eta^1{:}\eta^3$-bridged product **2e** or **3e**. The transformation of compound **2c** or **3c** into **2e** or **3e**, respectively, can occur by a twist about the bond between one metal and the central cumulene carbon, accompanied by bending back of the phosphines at the adjacent metal. However, the transformation of compound **2c** or **3c** into either **2d** or **3d** must occur by cumulene dissociation and subsequent attack at site 3 between the two carbonyls. Presumably, compounds **2d** and **3d** do not transform directly into the respective species **2e** and **3e**, since this would require substantial ligand reorganization. Instead, we propose a slow isomerization back to **2c** and **3c** by cumulene dissociation and recoordination, followed by isomerization to **2e** and **3e** as described above. Again, we have confirmed that cumulene dissociation is involved at some stage in the transformations involving **2c** and **3c** by the addition of methylallene and allene, respectively, generating mixtures of isomers of both compounds **2** and **3** in both cases.

Subsequent rearrangement of **2e** and **3e** to their respective vinylcarbene (allylidene) products **6** and **7a/b** occurs slowly at ambient temperature. We propose that this transformation occurs by migration of the adjacent methyl ligand to the central carbon of the bridging cumulene group in **2e** and **3e** to give an η^3-allyl intermediate (**A**) as shown in Scheme 8 (all ancillary ligands are omitted for clarity). This proposed methyl migration is supported by labeling studies in which it was established that the labeled methyl ligand in **2e** ended up exclusively as the methyl group in **6**. Rotation of the allyl group at one metal would bring the two ends of this group into the vicinity of the adjacent metal and C−H activation at either end of the monosubstitued allyl group (R=H) would yield **6**, while C−H activation at the less substituted end of the disubstituted allyl group (R = Me) would yield **7b**. However, in the transformation of **3e**, two isomers (**7a** and **7b**) are observed. We propose that the second isomer (**7a**) arises

via an η^1-allyl intermediate (**C**), as also diagrammed in Scheme 8. Rotation about the vinylic C−C bond followed by generation of the η^3-allyl species (**D**) results in an isomerization from a geometry in which both methyl substituents have a mutually *anti* arrangement to one in which they are *syn*. Carbon−hydrogen activation at the less substituted end of this allyl group would generate **7a**. The $\eta^3-\eta^1$ conversion is well documented in allyl complexes and is the process proposed for the facile equilibration often seen between *syn* and *anti* protons in these systems.[30] Although intermediate **C** has an η^1-allyl group that is bound to the metal via the more substituted carbon, this process cannot be unfavorable since **7a** is the more abundant isomer (in a 2:1 ratio). We suggest that this is due to more unfavorable interactions of the terminal methyl group in the product **7b** with the rest of the complex, since in this arrangement this methyl group is thrust into the vicinity of the metal−metal bond. In **7a** this methyl group avoids these unfavorable contacts. This was clearly demonstrated in the structure determination of the analogous $[Ir_2H(CO)_2(\mu\text{-}\eta^1\text{:}\eta^3\text{-}HCC(Et)C(H)Et)(dppm)_2][CF_3SO_3]$, in which the methyl groups of **7a** are replaced by ethyl substituents.[9] In this structure it is clear that the mutually *cis* arrangement of ethyl groups is favorable, while a *trans* arrangement (as in **7b**) would not be.

Conclusions

This study has established another example involving facile C−H activation of the methyl ligand in $[Ir_2(CH_3)(CO)(\mu\text{-}CO)(dppm)_2][CF_3SO_3]$ upon coordination of a ligand (in this case a series of cumulene molecules) at the adjacent metal. It also clearly demonstrates how ligand reactivity can change dramatically depending upon the ligand binding mode and the extent of involvement of the adjacent metal centers. Although with each cumulene investigated the cumulene is bound adjacent to an $Ir-CH_2$ bond in the kinetic product $[Ir_2H(\eta^2\text{-}H_2C{=}C{=}CRR')(CO)_2(\mu\text{-}CH_2)(dppm)_2][CF_3SO_3]$ (R, R′ = H, CH_3; R = R′ = H, CH_3, F), in no case does cumulene insertion into this $Ir-CH_2$ bond occur. Instead, as the temperature is increased, facile cumulene dissociation and recoordination at an alternate site is observed accompanied by regeneration of the methyl ligand from the methylene and hydride groups. Subsequent increases in temperature give rise to accompanying rearrangements which are more extensive for the allene and methylallene adducts than for the disubstituted cumulene adducts, which display similar although more limited reactivity owing either to steric or electronic effects. The detailed variable-temperature NMR study on the four cumulenes allows the identification of the cumulene coordination modes at different stages of the reactions and establishes that only the $\mu\text{-}\eta^1\text{:}\eta^3$-binding mode involving allene and methylallene results in coupling involving the methyl ligand accompanied by C−H activation of the resulting fragment. No other cumulene coordination mode resulted in ligand coupling, even when groups were adjacent. Neither the 1,1-dimethylallene nor the 1,1-difluoroallene ligands result in ligand coupling reactions since neither achieves the necessary $\mu\text{-}\eta^1\text{:}\eta^3$-coordination mode. The dimethyl-substituted molecule appears unable to access the bridging site owing to steric repulsion involving the methyl substituents, and the electronegative substituents on the difluoro analogue appear to favor bridging through the "$H_2C{=}C$" moiety, which is subsequently unreactive.

Acknowledgment. We thank the Natural Sciences and Engineering Research Council of Canada (NSERC) and the University of Alberta for financial support of the research and for scholarships (to D.J.A. and J.R.T.), and NSERC for funding the X-ray diffractometer. X-ray data for **2e** were collected by Dr. James F. Britten at McMaster University, Hamilton, ON, Canada.

Supporting Information Available: Tables of X-ray experimental details, atomic coordinates, interatomic distances and angles, anisotropic thermal parameters, and hydrogen parameters for compounds **2e** and **5c**. This material is available free of charge via the Internet at http://pubs.acs.org.

OM0580102

(30) (a) Corradini, P.; Maglio, G.; Musco, A.; Paiaro, G. *Chem. Commun.* **1966**, 618. (b) Vrieze, K.; Volger, H. C. *J. Organomet. Chem.* **1967**, *9*, 537. (c) Faller, J. W.; Thomsen, M. E.; Mattina, M. J. *J. Am. Chem. Soc.* **1071**, *93*, 2642. (d) Nixon, J. F.; Wilkins, B.; Clement, D. A. *J. Chem. Soc., Dalton Trans.* **1974**, 1993. (e) Osakada, K.; Chiba, T.; Nakamura, Y.; Yamamoto, T.; Yamamoto, A. *Organometallics* **1989**, *8*, 2602. (f) Consiglio, G.; Waymouth, R. M. *Chem. Rev.* **1989**, *89*, 257. (g) Solin, N.; Szabo, K. J. *Organometallics* **2001**, *20*, 5464.